Measurement 257 (2026) 118763

Contents lists available at ScienceDirect

Measurement

journal homepage: www.elsevier.com/locate/measurement

Advances and challenges in water leakage detection techniques for shield tunnels: a comprehensive review

Jundi Jiang [a,1], Yueqian Shen [a,*,1], Jinhu Wang [b], Jinguo Wang [a], Junjun Huang [a], Shihan Fu [a], Kai Guo [c], Vagner Ferreira [a]

[a] School of Earth Sciences and Engineering, Hohai University, Nanjing 211100, China
[b] Institute for Biodiversity and Ecosystem Dynamics (IBED), University of Amsterdam, Amsterdam 1012 WX, the Netherlands
[c] Guangdong Laboratory of Artificial Intelligence and Digital Economy (SZ), Shenzhen 518107, China

ARTICLE INFO

Keywords:
Shield tunnel
Water leakage
Review
Photogrammetry
LiDAR
Infrared thermal

ABSTRACT

Water leakage in shield tunnels presents significant challenges to the long-term stability and safety of underground infrastructure, making its effective detection imperative. In this context, data acquisition methods, including LiDAR (Light Detection and Ranging), photogrammetry, and thermal infrared imaging, have emerged as effective non-contact techniques for identifying water leakage. These modern sensing techniques offer substantial advantages over traditional manual inspection methods. However, the inherent characteristics of these sensors introduce specific challenges for water leakage detection, which hinder its effectiveness of tunnel and practical applications. This review examines recent methodologies designed to overcome these obstacles. It begins with an exploration of the three primary sensors utilized in tunnel water leakage detection. Then, representative techniques corresponding to each sensor are described, highlighting their potential and limitations, and qualitative analyses are incorporated to enhance understanding. To further address the lack of publicly available datasets, this review presents a novel LiDAR-acquired point cloud dataset specifically developed for tunnel water leakage detection, in addition to discussing existing photogrammetry-based datasets. The developed dataset comprises 4427 annotated leakage instances, totaling 22.71 million points, with an average point spacing of 2.1 mm. To the best of our knowledge, this is the first comprehensive review of tunnel water leakage detection and the first publicly available point cloud dataset dedicated to this task. This review provide an exhaustive analysis and discussion of the multifaceted aspects of tunnel water leakage detection, thereby assisting researchers in advancing the field and developing more effective detection and maintenance strategies.

1. Introduction

Shield tunnels represent an indispensable component of urban metro systems, providing reliable and efficient underground transit in urban areas [1]. However, these tunnels experience external loads and groundwater penetration that cause defects such as lining spalling [2,3], cracks [4,5], water leakage [6,7], and convergence deformation [8,9]. Water leakage is one of the most prevalent issues, and it poses significant threats to the structural integrity and operational safety. Therefore, regular inspection and periodic detection of tunnel water leakage are essential to maintain tunnel stability and safety.

Traditional methods for water leakage detection primarily rely on manual inspections, in which trained technicians visually inspect and record damaged lining segments. However, this approach suffers from several inherent limitations, including low efficiency due to limited inspection windows, high labor costs, and safety risks during operations in confined underground spaces [10]. Recent advancements in sensor techniques including LiDAR, photogrammetry, and infrared thermal imaging, offer promising alternatives for tunnel water leakage detection. Photogrammetry enables the generation of high-resolution imagery across extensive areas, providing a detailed visual record of the tunnel surface [11]. LiDAR captures tunnel geometry in three dimensions with millimeter-precision, making it indispensable for identifying structural deformations [1]. Meanwhile, infrared thermal imaging provides a non-

* Corresponding author.
E-mail addresses: jdjiang@hhu.edu.cn (J. Jiang), y.shen_lidar@hhu.edu.cn (Y. Shen), jinhu.wang@hotmail.com (J. Wang), wang_jinguo@hhu.edu.cn (J. Wang), hjj_lidar@hhu.edu.cn (J. Huang), nothanfu0228@gmail.com (S. Fu), guokai@gml.ac.cn (K. Guo), vagnergf@hhu.edu.cn (V. Ferreira).
[1] Jundi Jiang and Yueqian Shen are the co-first authors.

https://doi.org/10.1016/j.measurement.2025.118763
Received 16 March 2025; Received in revised form 4 August 2025; Accepted 18 August 2025
Available online 21 August 2025
0263-2241/© 2025 Elsevier Ltd. All rights are reserved, including those for text and data mining, AI training, and similar technologies.

invasive means of identifying water leakage by detecting thermal anomalies caused by moisture, even when water leakage is hidden beneath the surface [12].

A key issue in detecting tunnel water leakage is extracting features from sensor measurements. However, the irregular shapes of water leakage patterns, coupled with environmental noise and potential occlusions, present significant challenges. Isolating these features is challenging due to the low resolution, noise interference, environmental complexity, feature similarity, and occlusions. Additionally, each type of sensor introduces its own set of limitations. As a result, the task of automatically detecting water leakage from sensor data has garnered increasing attention in recent research. This review critically examines the state-of-the-art methodologies of tunnel water leakage detection using data from various sensors. To the best of our knowledge, this is the first review to cover multiple sensor technologies for tunnel water leakage detection. Furthermore, a thorough assessment of the potential and limitations of these methodologies is provided through qualitative analyses. Additionally, to bridge the gap in publicly available point cloud datasets, we introduce the first open-access LiDAR-based point cloud dataset specifically designed for tunnel water leakage detection. This dataset complements existing photogrammetry datasets, offering valuable resources for the development and benchmarking of new detection algorithms.

The remainder of this paper is illustrated in Fig. 1, with the specific content outlined as follows: Section 2 presents a scientometric analysis of the selected literature. Section 3 reviews the fundamental principles and components of the various detection systems utilized in the field of tunnel water leakage detection. Section 4 introduces the publicly available datasets derived from photogrammetry sensors, along with the newly released LiDAR-based point cloud dataset specifically designed for tunnel water leakage detection. Section 5 outlines state-of-the-art automatic detection methods. Section 6 highlights key findings, discusses the strengths and limitations of different feature extraction methods, and provides an in-depth analysis of the future work. Finally, Section 7 concludes the study by summarizing the contributions and outlining potential directions for further research.

2. Scient metric analysis of selected papers

2.1. Literature search and screening

We performed a systematic literature search on the Web of Science Core Collection to analyze the methods for shield-tunnel water leakage detection. Additionally, Google Scholar was used to broaden the scope of this study. The search process followed a structured approach: first, the Web of Science Core Collection was queried using the keywords “leakage”, “seepage”, and “moisture”. Next, the abstracts of the retrieved papers were manually reviewed to check their relevance and quality. The identical query was then executed in Google Scholar to capture studies not indexed by Web of Science. The search was limited to publications from 2014 to 2025, and restricted to the subject categories “Engineering”, “Materials Science”, “Construction Building Technology”, and related fields. Studies that did not focus specifically on shield tunnel water leakage detection (e.g., investigations in horseshoe-shaped or non-shield tunnels) were excluded. Through this rigorous screening process, a total of 105 papers were selected for review.

2.2. Interannual distribution of literature

Fig. 2 presents the annual distribution of selected studies on shield tunnel water leakage detection over the interval 2014–2025. During the formative period of 2014–2016, publication output remained minimal (1–2 articles per year), reflecting early exploratory efforts. This was followed by a moderate increase to 5 and 6 articles in 2017 and 2018, respectively, then decline to 3 articles in 2019. Thereafter, the discipline experienced pronounced expansion: 15 publications appeared in 2020, rising to 22 in 2021. The count decline to 12 articles in 2022, but then reach to a peak of 23 in 2023 and stayed high at 20 in 2024. Preliminary data for 2025 indicate that this upward trajectory persists. This growth trend highlights the increasing emphasis on advanced sensing techniques, improved data-processing algorithms, and integrated monitoring strategies for reliable shield-tunnel water leakage detection.

2.3. Analysis of keywords co-occurrence

To identify research hotspots in tunnel water leakage detection, we analyzed the co-occurrence of keywords with VOSviewer, where the RIS files of the collected literature were imported for analysis. We selected keywords with more than three occurrences, excluding redundant synonyms to maintain clarity. As depicted in Fig. 3, each node in the network represents a keyword, with the node size corresponding to its occurrence; larger nodes indicate higher frequencies. The edges depict relationships between nodes, with the link strength represented by the total length of its connected edges. Additionally, different colors distinguish clusters of related research themes.

The analysis reveals that “deep learning” is the most frequently appearing term, highlighting the predominant role of deep learning methods in tunnel water leakage detection. Additionally, the high frequency of the keyword “crack detection” indicates that structural cracks continue to pose critical challenges in tunnel maintenance. Furthermore, yearly keyword trends reveal that the term “laser scanning” (and related phrases such as “point cloud”) has exhibited steadily increasing prominence since 2020, reflecting growing use of 3D sensing for water leakage detection. Moreover, the rise of “lightweight” shows a shift toward resource-efficient, real-time monitoring systems alongside high detection accuracy.

3. Systems for tunnel water leakage detection

3.1. Photogrammetry-based systems

Photogrammetry-based systems provide an advanced and efficient approach for tunnel inspections by capturing detailed images. These systems are particularly effective in identifying surface defects such as cracks [4,5,13] and water leakage [10,14,15]. One of the primary advantages of photogrammetry is its non-invasive nature, enabling data collection without physical contact with tunnel structures. This ensures structural integrity while facilitating accurate defect identification and measurement. These systems generally consist of three components: an image acquisition system, a control system that processes and synchronizes data, and a motion control unit for regulating camera movement to ensure stable imaging (Fig. 4).

Photogrammetry-based systems use machine vision sensors, such as line-scan or area-scan CCD cameras. Area-scan CCD cameras are susceptible to image distortion [16], while linear CCD cameras provide more stable imaging under uneven tunnel conditions. Additionally, tunnel environments often suffer from poor lighting, necessitating LED illumination to ensure clear and consistent image quality. Another critical factor in photogrammetry-based inspection is speed. High speeds can lead to motion blur or distortion [15], while lower speeds enhance image quality but prolong data collection. Striking an optimal balance between speed and accuracy is essential for effective tunnel inspections.

Building upon these considerations, Researchers have developed photogrammetry-based inspection systems such as the MTI-100 [16], MTI-200a [17], and MTSIS [18]. These systems, summarized in Table 1, exhibit a range of technical specifications, such as inspection speeds, image resolutions, and coverage capabilities. Their successful implementation has resulted in high-quality datasets, significantly advancing water leakage detection methodologies. Integrating advanced imaging techniques has improved defect detection accuracy and the efficiency of inspection workflows.

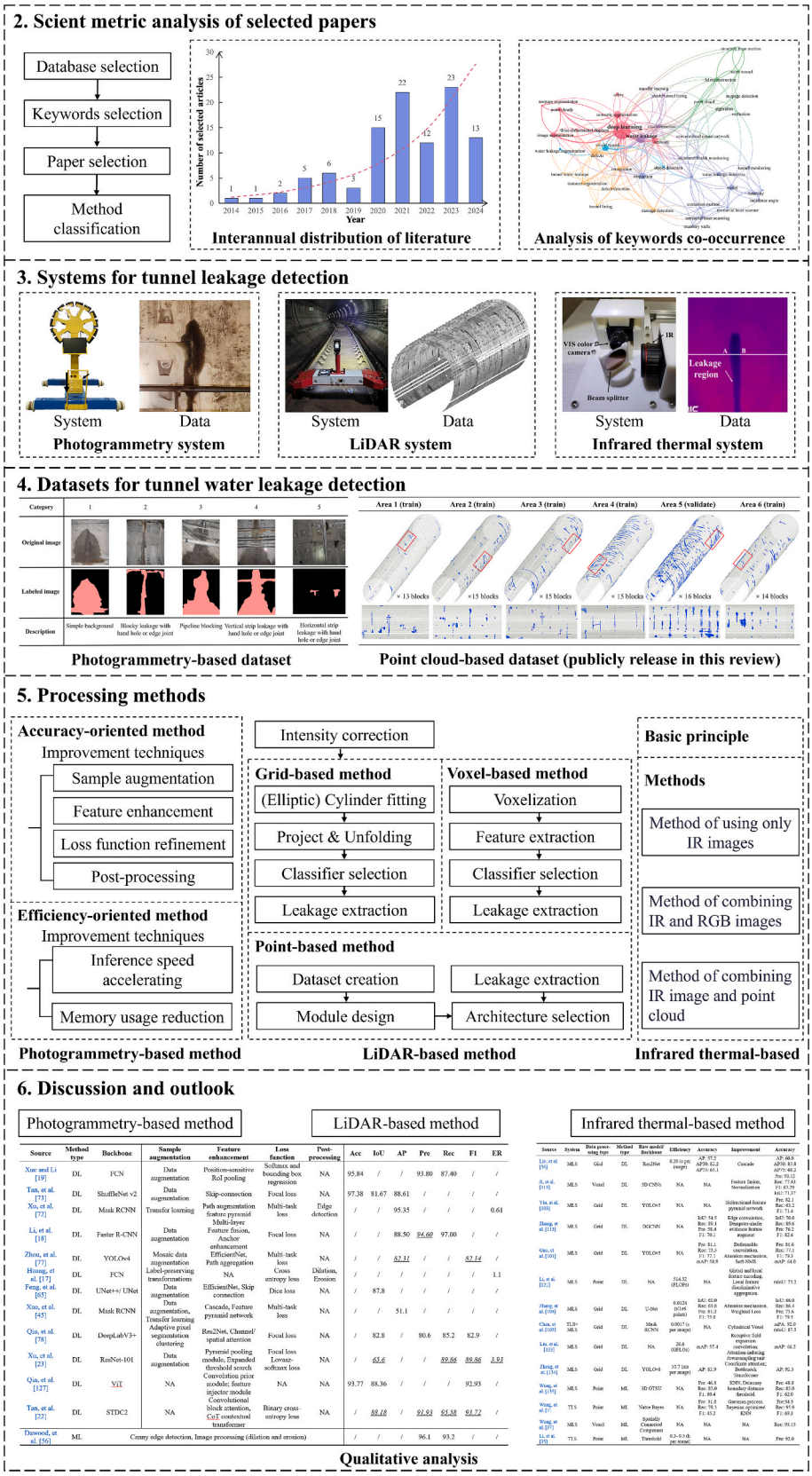

Fig. 1. The pipeline of the review.

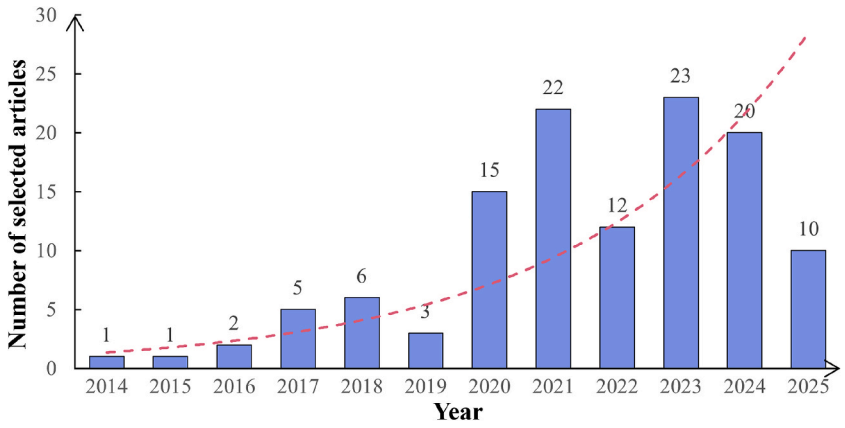

Fig. 2. Number of literature and trends of shield tunnel water leakage detection from 2014 to 2025.

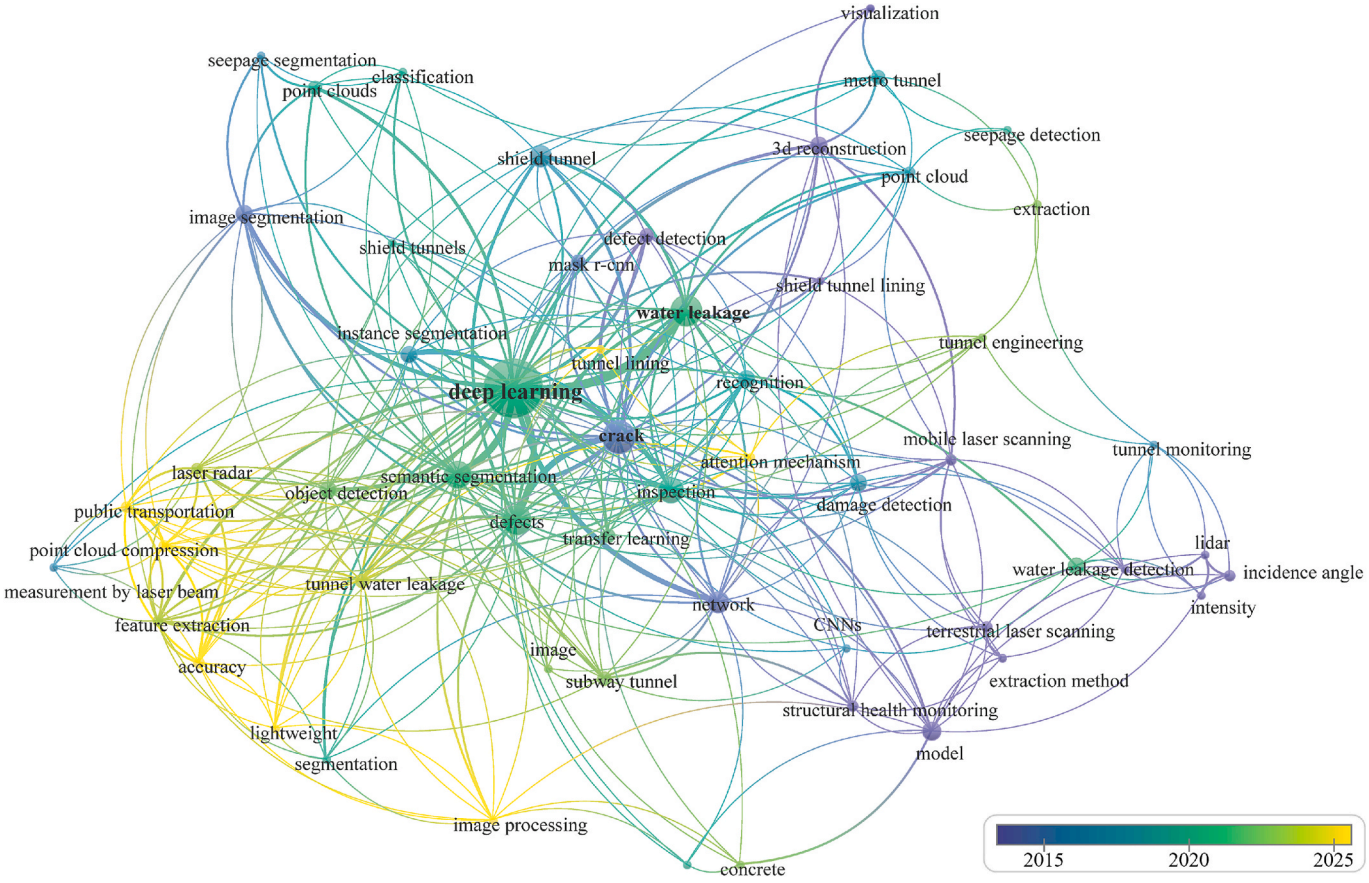

Fig. 3. Network of keywords co-occurrence.

3.2. LiDAR-based systems

LiDAR technique provides high resolution 3D measurements, outperforming traditional inspections in complex tunnel scenarios [25]. These systems can be broadly categorized into two main types: Terrestrial Laser Scanning system (TLS) and Mobile Laser Scanning system (MLS).

3.2.1. Terrestrial laser scanning (TLS)

TLS is a ground-based technique for high-precision 3D measurement, which has been applied in landscape mapping [26], structural monitoring [27], and 3D modeling of built environments [28]. A LiDAR scanner, mounted on a stable tripod, emits laser pulses toward the target. The system measures the time-of-flight or phase shift of reflected pulses to calculate distances and construct a detailed 3D map. This approach achieves millimeter accuracy, enabling detection of small tunnel deformations [29].

In shield tunnels, the LiDAR scanning positions are placed at intervals to record surface conditions, as shown in Fig. 5. By scanning from multiple positions, TLS collects detailed 3D point cloud data. However, point density decreases with distance from the scanner, with closer areas containing more points and finer details, and distant areas having fewer points and lower accuracy, as shown in Fig. 6. Therefore, point cloud registration is required to align and merge multiple scans [30–32]. However, complex tunnel geometries complicate registration, necessitating advanced algorithms and precise calibration to reduce errors.

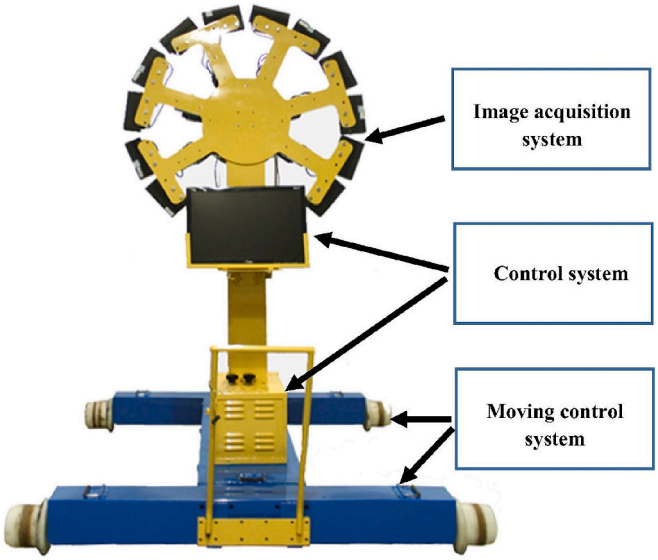

Fig. 4. The general composition of photogrammetry-based systems. [16].

Moreover, the requirement for fixed-station operation results in slower data collection, making it less efficient for large-scale or repeated scans.

3.2.2. *Mobile laser scanning (MLS)*

MLS integrates LiDAR sensors with mobile platforms such as vehicles, trolleys, or backpacks, for continuous data collection. Compared to TLS, MLS provides enhanced mobility and higher scanning speeds, making it suitable for autonomous driving [34], urban mapping [35,36], and power assets monitoring [35].

In shield tunnels, the MLS system typically deploys LiDAR sensors mounted on a rail trolley, reducing manual effort while ensuring precise data collection. A typical MLS setup includes a LiDAR scanner, an odometer, track sensors, an Inertial Measurement Unit (IMU), and the trolley platform. As the trolley moves along the tunnel track, it scans the tunnel to acquire high-density 3D point clouds. Several studies have developed specialized MLS systems for tunnel inspections [37–40], as shown in Fig. 7. Maintaining a constant distance between the trolley and the lining yields near-uniform point density, as shown in Fig. 8. Additionally, MLS significantly reduces inspection time while preserving high accuracy, making it particularly effective for large-scale tunnel projects.

3.3. *Infrared thermal-based systems*

Infrared thermal sensors, also known as thermal imaging sensors, detect infrared radiation (heat) emitted by objects. As all objects emit infrared radiation, the emitted energy can be resolved into temperature variations or thermal images [42]. Thermal sensors can detect slight temperature variations without external lighting, making them valuable for applications such as defect detection [12,43], electrical equipment monitoring [44].

In shield tunnels, infrared thermography detects water leakage through surface-temperature anomalies. These sensors are often combined with RGB cameras to improve detection accuracy and compensate for their limitations, as demonstrated in Fig. 9 [42]. The presence of water leakage often results in localized temperature differences, which are captured by the thermal sensor [45]. These anomalies can indicate potential water leakage points, enabling early detection and intervention. However, ambient temperature, humidity, and airflow can distort thermal readings, leading to false positives or undetected water leakages. Additionally, thermal image interpretation requires expertise, as temperature variations may stem from material heterogeneity or external heat sources.

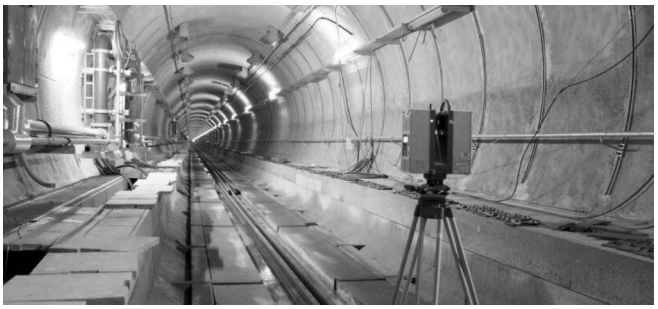

Fig. 5. Terrestrial laser scanner shield tunnel data collection [33].

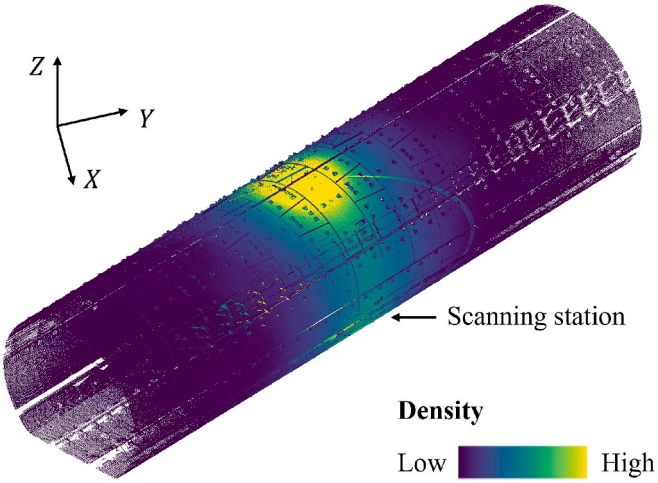

Fig. 6. Point cloud data obtained by TLS.

Table 1
Technical specifications of the photogrammetry-based systems for tunnel inspection.

Authors (Year)	System name	Visual system composition	Image size	Image resolution	Inspection speed	Inspection range
Huang, et al. [16], Xue and Li [19]	MTI-100	6 linear CCD cameras	3,000 × 3,724	0.3 mm/pixel	3–5 km/h	270°
Huang, et al. [17], Zhao, et al. [20], Zhao, et al. [21], Tan, et al. [22]	MTI-200a	6 linear CCD cameras	3,000 × 24,576	0.2 mm/pixel	0–10 km/h	270°
Li, et al. [18]	MTSIS	8 linear CCD cameras	20,000 × 20,000	0.2 mm/pixel	5–10 km/h	280°
Xu, et al. [23]	–	6 area-array CCD cameras	4,112 × 3,008	0.5 mm/pixel	0–20 km/h	250°
Wu and Guo [24]	MS100	–	16,327 × 8623	–	–	360°
Wang, et al. [14]	–	8 area-array CCD cameras	4,096 × 2,168	0.4 mm/pixel	5–15 km/h	260°

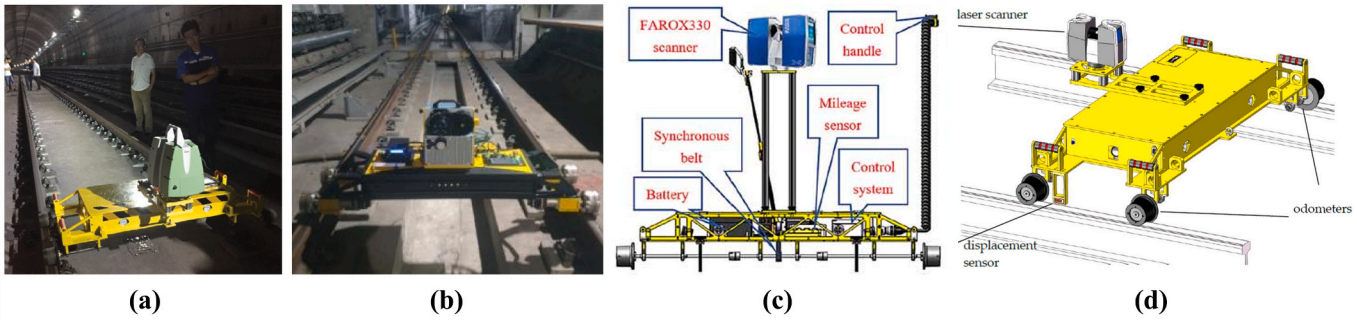

Fig. 7. Structure of mobile LiDAR systems. (a) [38]; (b) [39]; (c) [40]; (d) [41].

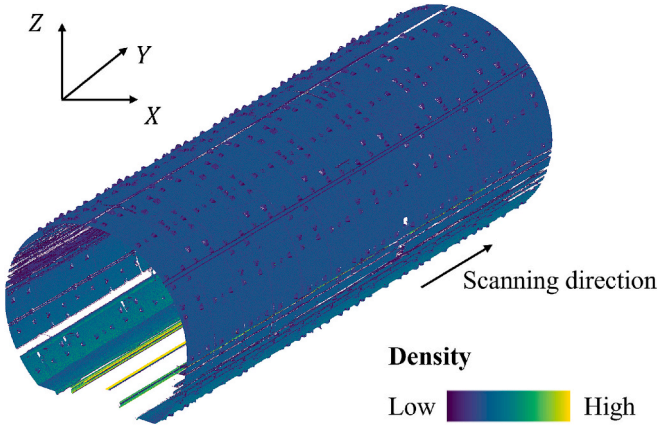

Fig. 8. Point cloud data obtained by MLS.

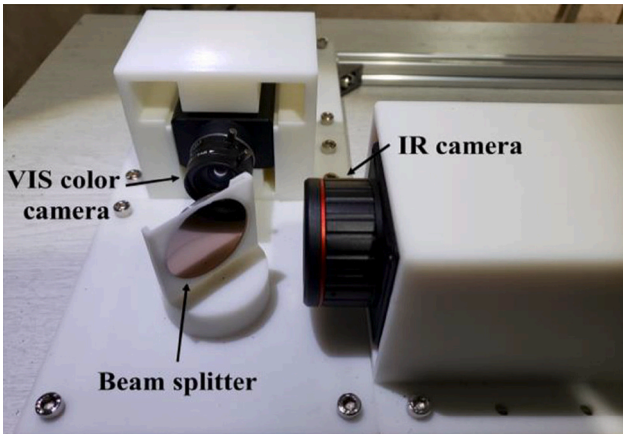

Fig. 9. RGB camera and IR camera integrated data collection system [42].

3.4. Synchronous acquisition control system

Current sensing techniques, including Photogrammetry, laser-scanned point clouds, and infrared thermal imaging, each reveals specific defect types, such as surface detail and cracks, precise 3D geometry, and subsurface moisture patterns. However, any technique cannot provide complete assessment. This limitation is driving development of multi-sensor systems that combine these complementary detection capabilities.

Sun, et al. [46] designed a synchronized acquisition network of several devices, including line-array cameras, laser scanners, infrared imagers and ground-penetrating radar. An encoder generates trigger pulses in both TTL and differential formats. A main controller timestamps and tallies these pulses, then transmits the data via TCP/IP to a host computer. A server-client software layer issues uniform start, pause, resume and stop commands and consolidates data from acquisition nodes. To correct cumulative encoder drift without external markers, the system detects tunnel ring joints in the point cloud using circle fitting, two-dimensional projection and sliding-window constraints. Field experiments have demonstrated the accuracy improvements from tens of meters to less than one meter, and reached a relative positioning accuracy of approximately 0.1 % in operational tunnel environments.

4. Datasets for tunnel water leakage detection

4.1. Photogrammetry-based dataset for water leakage detection

To the best of our knowledge, there is only one publicly available dataset specifically designed for tunnel water leakage detection. This dataset [47] comprises high-resolution (2330 × 1747) images captured from various shield tunnels located in Shanghai, China. Some sample images from the dataset are presented in Fig. 10 [48]. These images were collected under various environmental conditions and represent a wide range of tunnel lining defects.

The dataset consists of 911 images, systematically divided into 711 images for training and 200 images for validation. The dataset is categorized into five distinct types by their characteristics: simple background, blocky leakage with hand hole or edge joint, pipeline blocking, vertical strip leakage with hand hole or edge joint, and horizontal strip leakage with hand hole or edge joint, as illustrated in Fig. 10. This class structure ensures diversity and supports reliable model training.

To enhance the robustness and generalizability of machine learning models trained on this dataset, data augmentation techniques were applied. These techniques included: (1) noise injection, Gaussian and salt-and-pepper noise were introduced to simulate real-world variation. (2) geometric transformations, rotating and scaling images to increase viewpoint diversity. As a result of these augmentations, the dataset was expanded fivefold, increasing from 911 to 3555 images. The dataset is freely available for download at https://doi.org/10.17632/xz2nykszbs.1. This dataset provides researchers with well labeled water leakage samples for training and testing automatic water leakage detection models under realistic tunnel conditions.

4.2. Point cloud-based dataset for water leakage detection

While photogrammetry-based datasets have advanced research on tunnel water leakage detection, publicly accessible point-cloud datasets remain unavailable for this application. To this end, we developed and released a point cloud dataset for 3D water leakage detection.

The point cloud data was collected in June 2023 along Nanjing Metro Line 2, spanning from Jiqingmen Street station to Xinglong Street station. The tunnel overburden in this section ranges from 12.00 m to

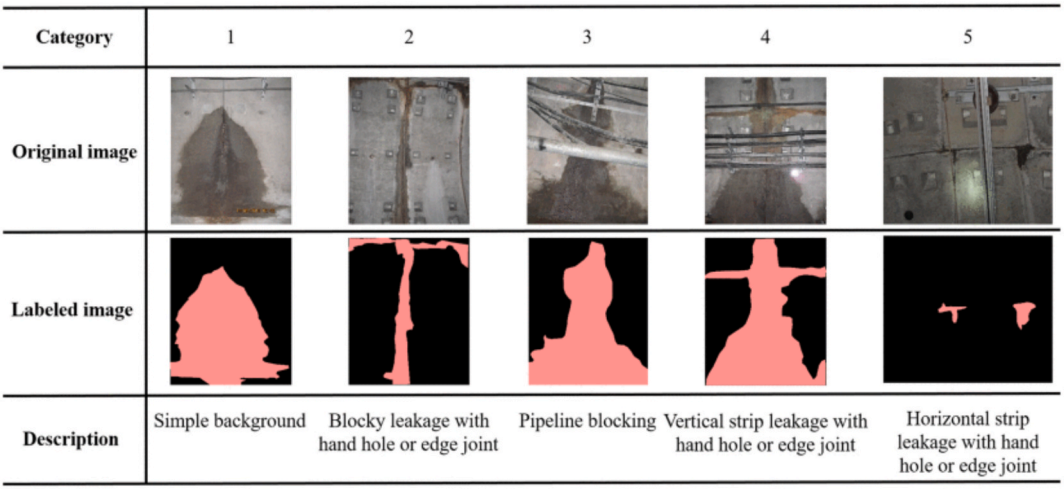

Fig. 10. Sample of water leakage in shield tunnel with different scenarios (black/red signifies the background/foreground) [48]. (For interpretation of the references to color in this figure legend, the reader is referred to the web version of this article.)

20.00 m. The terrain lies on the Lower Yangtze River alluvial plain, with soils mainly composed of clay, silty clay, silt, and sand. Groundwater levels fluctuate between 1.50 m and 2.60 m below the ground surface, with an annual amplitude of approximately 0.5 m. Additionally, the tunnel was constructed using the conventional shield-driven method and lined with prefabricated concrete segmental rings. The dataset covers approximately 2 km of tunnel length, ensuring diverse environments conditions for a more representative and robust dataset. Data acquisition was performed using an MLS equipped with a FARO Focus3D 330 laser scanner, which features an angular resolution of 0.009° and a ranging error of ±2 mm. A panoramic scanning approach was adopted to ensure comprehensive spatial coverage. This resulting point cloud data has an average point space of 2.1 mm, providing high-resolution spatial information crucial for accurate detection.

To enhance the quality and utility of the dataset, the raw point cloud data underwent a structured preprocessing and annotation workflow: (1) Noise removal: eliminating extraneous data to enhance clarity. (2) Exclusion of auxiliary structures: filtering out pipes, cables, and other non-structural elements to minimize interference. (3) Manual annotation: water leakage instances such as visible wet stains and water leakage were labeled using field-captured photographs as references to ensure precise visual alignment. (4) Intensity-based refinement: A 95 % confidence interval was applied to filter erroneous annotations, improving reliability by eliminating misclassified points.

The dataset adopts the Stanford Large-Scale 3D Indoor Spaces Dataset (S3DIS) [49] format. The point cloud data was divided into six distinct areas, with each area was further segmented into 15-meter tunnel blocks to prevent memory overflow during model training. As shown in Fig. 11, Area 5 serves as validation set, while the remaining five Areas are allocated for training purposes. The dataset contains 4427 annotated water leakage instances, which collectively span 22.71 million points (approximately 1.5 % of the total dataset). The background class consists of 1489.01 million points, which is 65 times the number of water leakage sample points.

The dataset is provided in text (.txt) format, each file includes 3D coordinates and intensity values. The dataset is released under the MIT license for academic and commercial use with attribution. We also provide a down-sampled version of the S3DIS-Leakage dataset. The down-sampled dataset is generated using a spatially uniform distance-based sampling method, which preserves the original geometric distribution and water leakage spatial patterns while significantly reducing computational demands. Specifically, the average point spacing is reduced from 2.1 mm to 10 mm, achieving an 85 % storage reduction. The dataset can be freely downloaded from www.kaggle.com/datasets/yueqianshen/s3dis-leakage.

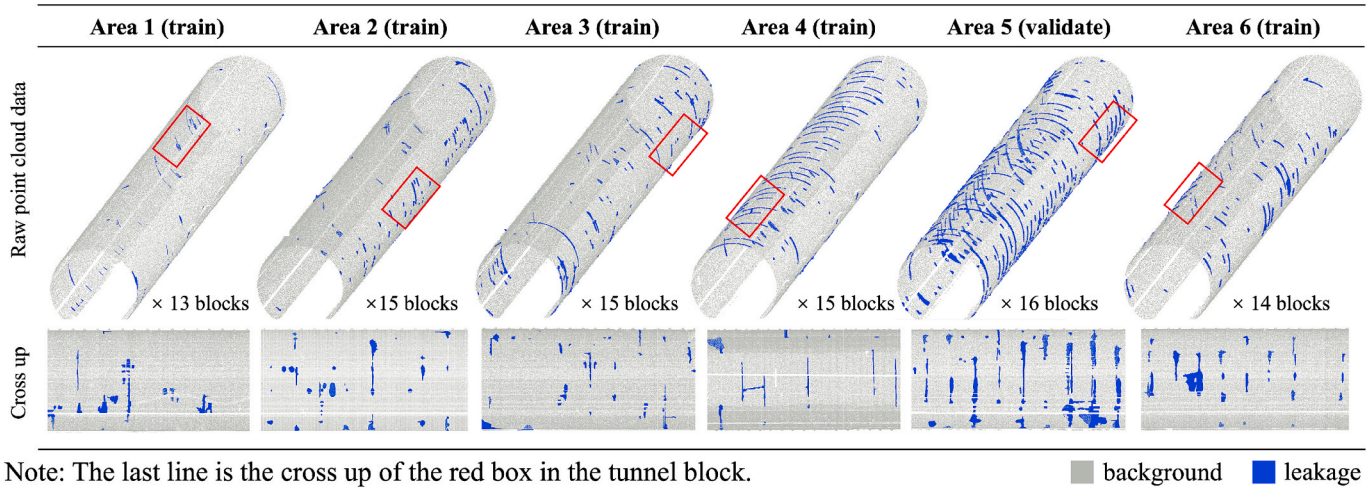

Fig. 11. S3DIS_leakage dataset.

5. Processing methods

5.1. Photogrammetry-based water leakage detection methods

Photogrammetry has become an essential tool in tunnel inspection, particularly for detecting defects such as water leakages, cracks [50–52] and lining spalling [53,54]. Water leakage is the most prevalent and one of the most challenging detect [15,55]. Photogrammetry-based methods identify water leakage patterns on linings and enable early detection of potential water leakage.

Advanced image processing techniques have significantly improved the accuracy and reliability of identifying water leakage areas. Edge detection algorithms, such as the Canny [56] and Sobel [57], have proven effective in delineating water leakage regions by detecting variations of image pixel that correspond to the edges of wet areas on tunnel linings. Dawood, et al. [58] utilized the Canny edge detection algorithm to enhance the clarity of water leakage boundary edges. They further applied morphological operations such as dilation and erosion to improve boundary definitions and clarify visual distinctions. Additionally, adaptive thresholding techniques, such as the OTSU [59], play a crucial role in distinguishing water leakage areas from the background. This method automatically determines the optimal threshold by maximizing the variance between water leakage and dry regions [16]. However, these traditional image processing techniques still face challenges in lighting variations, surface textures, and noise interference [60].

Given the limitations of traditional image processing methods, deep learning has emerged as a powerful alternative, offering superior adaptability and robustness in challenging tunnel conditions [11,61]. Deep learning models can automatically learn and extract features from datasets, significantly enhancing detection accuracy and reliability. Several state-of-the-art deep learning architectures have been widely adopted for tunnel water leakage detection, including Fully Convolutional Networks (FCN) [62], You Only Look Once (YOLO) [63], DeepLabv3+ [64], Mask R-CNN [65], and Faster R-CNN [66]. The general workflow of deep learning methods for water leakage detection using photogrammetry-generated data is illustrated in Fig. 12.

Deep learning for tunnel water leakage detection targets two main challenges: achieving high detection accuracy and enhancing computational efficiency for real-time applications or resource-constrained environments. To address these challenges, researchers have explored various backbone networks and introduced specific modules designed to enhance either accuracy or efficiency, which can be broadly classified into two categories: **Accuracy-oriented methods** and **Efficiency-oriented methods.**

5.1.1. Accuracy-oriented methods

Accuracy-oriented methods focus on maximizing detection precision, ensuring the identification of small, intricate, or complex water leakage patterns. Early recognition of such minor water leakages both prevents deterioration and informs maintenance planning. These methods refine model architecture and training data to improve detection accuracy, including enhancing feature representation, increasing model capacity, and optimizing output quality. Efforts to achieve higher accuracy have been made from four key perspectives:

(1) Sample augmentation

Photogrammetry datasets for tunnel water leakage detection often lack diversity and variability in lighting, angles, and textures [17,67,68]. Collecting diverse samples with various lighting conditions, angles, and surface textures is difficult. This scarcity of diverse training samples may lead to overfitting [47,69]. Data augmentation simulates real-world variations to adapt to different conditions [18].

Fig. 13 summarizes common augmentation techniques in water leakage detection: (1) Geometric transformation: rotations, cropping, scaling, and flipping help the model become invariant to changes in orientation and viewpoint [21]. (2) Photometric adjustments: noise injection, brightness and contrast alterations simulate different lighting conditions, enabling the model to be more robust in detecting water leakages under varying circumstances [20,70,71]. Lin, et al. [72] introduced an ALTM low-light image enhancement followed by CLAHE for adaptive equalization adjustment. (3)Advanced augmentation techniques: Chen, et al. [48] proposed a hybrid augmentation approach combining Mixup and Mosaic techniques.

Additionally, transfer learning leverages pre-trained models that have learned generalized features from large-scale datasets, which is beneficial when domain-specific datasets are limited or lack diversity [47,68]. Knowledge transfer from pre-trained models imparts core object detection capabilities, improving generalization in tunnel water leakage detection [73]. Many studies have employed pre-trained model weights from the COCO dataset to reduce the need for large domain-

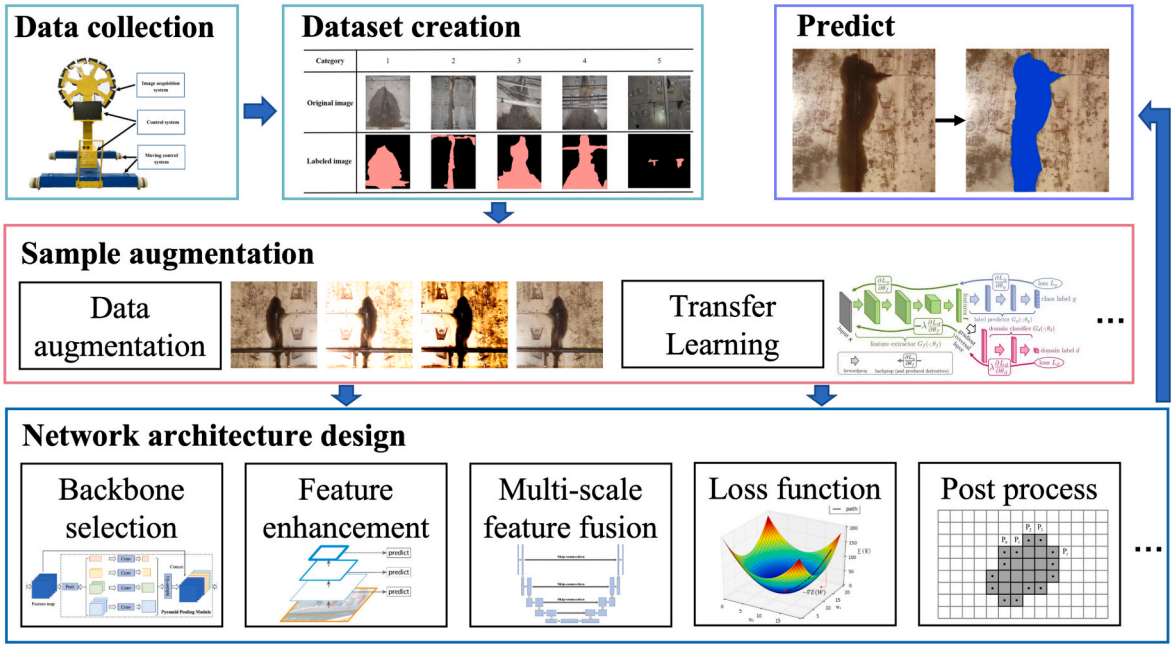

Fig. 12. General workflow of deep learning methods for water leakage detection based on photogrammetry-generated data.

Fig. 13. Data augmentation techniques.

specific datasets and shorten training time. While the COCO dataset lacks water leakage-specific images, its pre-trained weights allow models to learn fundamental object detection principles [21,70].

(2) Feature enhancement

In deep learning models, shallow feature maps capture fine-grained details from input images, while deeper layers extract more abstract features. However, as the network deepens, detailed local information may be lost, making it difficult to detect both small-scale details and complex patterns. To address this, researchers introduced feature enhancement modules to preserve local details and integrate global context. Key enhancement techniques include multi-scale feature fusion [18,23], attention mechanisms [22], and context-aware modules [23,74]. One critical approach is the use of skip connections, which retain spatial details by bypassing intermediate layers, as shown in Fig. 14(a) [67,75]. Dense skip connections promote feature reuse across layers, enhancing multi-scale fusion and detection accuracy, as presented in Fig. 14(b). These approaches improve gradient flow, mitigate vanishing gradients, and capture details at multiple scales, thereby enhancing detection accuracy.

The cascade strategy refines feature extraction in multiple stages, ensuring a hierarchical representation of water leakage patterns [47,68,73]. Fig. 15 illustrates the workflow of applying the cascade strategy in the Mask R-CNN model. This strategy operates by organizing the model into multiple stages, where each successive stage builds upon the features extracted in the previous stage. The early stages focus on capturing basic, low-level features, while later stages progressively handle more abstract and complex patterns. This hierarchical approach allows the model to refine its understanding at each stage, leading to more detailed and accurate representations of water leakage patterns. Pyramid Pooling Module (PPM) introduced in PSPNet [76,77] further enhance feature extraction by multi-scale feature extraction [22,23]. PPM aggregate multiple receptive fields features to enhance the model's capacity to detect tunnel water leakage patterns of varying scales, as shown in Fig. 16. Building on this, Xu, et al. [74] introduced the Path Aggregation Feature Pyramid Network (PAFPN), which improves feature extraction by adding a bottom-up path for low-level features. Additionally, Wang, et al. [14] proposed the Bi-directional Feature Pyramid Network (Bi-FPN), which employs bi-directional feature fusion to enhance multi-scale water leakage detection, particularly improving boundary accuracy. Another effective approach involves expanding the receptive field to capture more global information. Wang, et al. [14] proposed the Non-Local Block, which expands the receptive field and improves the model's ability to perceive water leakage regions on a global scale, particularly in the lower feature layers.

Additionally, attention mechanisms have emerged as a crucial strategy for feature enhancement. These mechanisms allow the model to

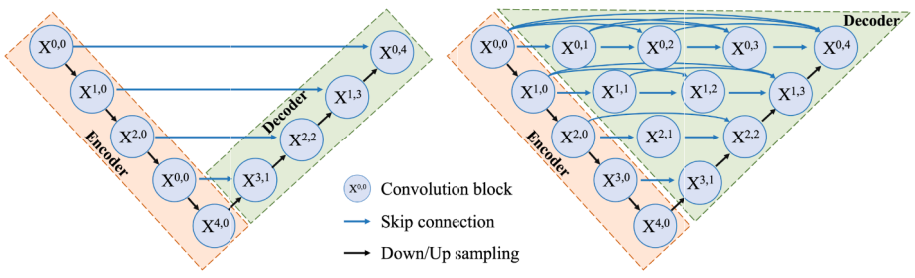

(a) skip connection architecture (b) dense skip connection architecture

Fig. 14. Architecture of skip connection and dense skip connection.

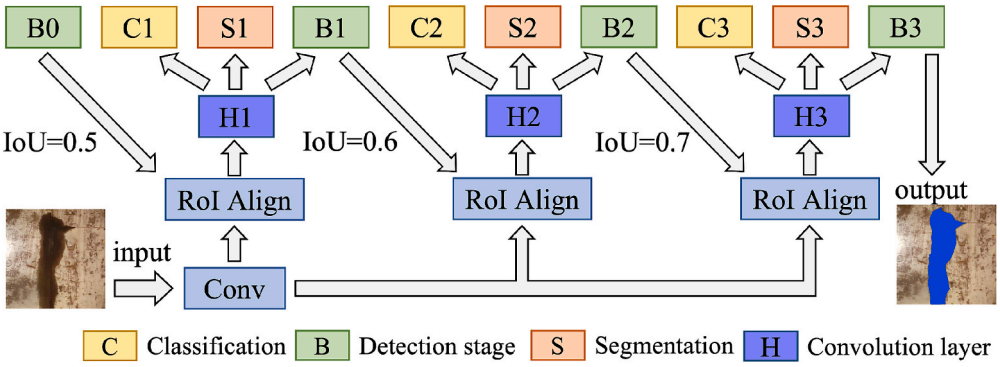

Fig. 15. Workflow of applying the cascade strategy in a Mask R-CNN model.

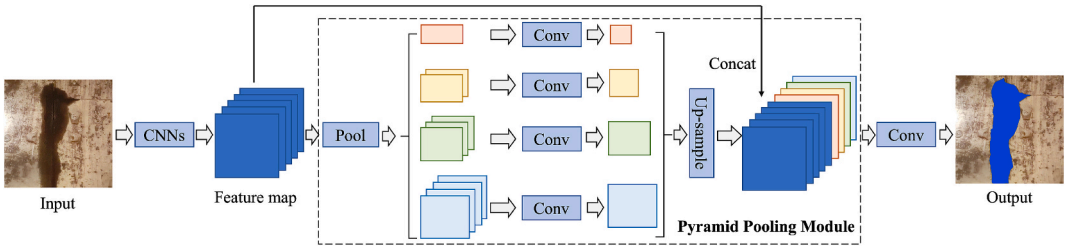

Fig. 16. Workflow of Pyramid Pooling Module (PPM).

focus on the key features while suppressing irrelevant information, improving its ability to detect subtle and complex water leakage patterns. For instance, some researchers have utilized the SENet module in EfficientNet [78] to enhance the importance of key feature channels, thereby improving the semantic representation of defects and suppressing interference from complex tunnel backgrounds [79].

(3) Loss function refinement

The loss function measures differences between predictions and ground truth and directs model optimization. However, in tunnel water leakage detection tasks, sample imbalance presents a major challenge. Water leakage regions typically occupy a small fraction, while non-leakage areas dominate the dataset. This imbalance biases model training as the loss is dominated by the majority background samples. Consequently, the model may struggle to detect small or subtle water leakage patterns, as these minority samples are underrepresented in the optimization process.

To address this issue, researchers have introduced refined loss functions that mitigate class imbalance. Refined loss functions emphasize minority water leakage samples over the majority background class. Tan, et al. [75] and Qiu, et al. [80] applied Focal Loss to reduce the influence of the majority class (background) and encourage the model to focus on water leakage areas that are more difficult to detect. Wang, et al. [71] further combined Dice Loss and Focal Loss to address the issue of class imbalance caused by the low proportion of water leakage pixels. Additionally, Zhao, et al. [20] proposed a multi-task loss function, which integrates classification loss, bounding box regression loss, and mask loss. This multi-task loss improves both water leakage detection and segmentation accuracy, enhancing defect localization.

(4) Post-processing

Post-processing optimizes segmentation and suppresses noise to ensure more reliable predictions. In tunnel water leakage detection, inaccurate defect edges localization reduces compromise the segmentation precision. To address this, researchers proposed to incorporate an edge detection branch into the network architecture. The branch uses the Sobel operator to extract defect edges and incorporates them into the loss function [48,74]. Following edge detection, morphological operations, such as dilation and erosion, are employed to remove noise and improve region continuity, ensuring clearer segmentation [17]. Additionally, the curved tunnels introduce distortions for accurate prediction in tunnel water leakage detection. To this end, a cylindrical projection model was used to correct perspective distortions through projection alignment, enabling more precise detection of water leakage patterns by adjusting the structure into a more interpretable form [81].

In conclusion, accuracy-oriented methods advanced water leakage detection by focusing on precise detection of leakage patterns. These methods address the inherent challenges of tunnel environments, such as limited data diversity, complex geometries, and class imbalance, through strategies that enhance model generalization and robustness. Sample augmentation, feature enhancement, loss refinement, and post-processing help models distinguish fine-grained water leakage against complex backgrounds. Their emphasis on precision supports early-stage water leakage detection and maintenance planning, enhancing tunnel safety and lifespan.

5.1.2. Efficiency-oriented methods

Efficiency-oriented methods in tunnel water leakage detection focus on optimizing the computational performance to enable real-time detection and reduce resource use. These methods are particularly crucial for real-time monitoring systems and resource-constrained environments, such as mobile devices, embedded systems, and edge computing platforms [18]. By prioritizing efficiency, these approaches can run on standard hardware without sacrificing detection speed. Efficiency in this context primarily addresses two key aspects, including inference speed and memory usage. Inference speed refers to how quickly the model can process data, which is essential for real-time applications. Memory usage denotes memory footprint and computational load of the model [82].

(1) Inference speed optimization

Traditional deep learning models with millions of parameters and complex operations result in slow processing times that hinder real-world deployment. To this end, researchers developed several optimization techniques aimed at accelerating inference speed while maintaining detection accuracy.

One effective strategy is lightweight architectures that cut

complexity reduce model complexity while preserving performance. ShuffleNet v2 [83] introduces a channel shuffle operation and a branch-based architecture that efficiently distributes computations across feature maps, significantly reducing inference time [75]. Depthwise Separable Convolution (DSC) employed in models like YOLOv4, YOLOv7 [84,85], decompose convolutions to cut parameters and speed up computation [67,79]. EfficientNet further refines inference speed through a compound scaling strategy, which adjusts model depth, width, and resolution in a balanced manner to achieve a trade-off between speed and feature extraction [67].

(2) Memory usage

Existing models are memory-intensive, limiting their usability for real-time detection tasks in resource-constrained environments. Several strategies have been developed to optimize memory usage in tunnel water leakage detection models.

One effective approach is pruning unnecessary model parameters, eliminating redundant computations. Xue, et al. [68] proposed a parameter pruning technique that removes redundant connections, which can reduce both memory usage and computation load. This is particularly beneficial for long-tunnel monitoring, where hardware constraints are common. Depthwise Separable Convolutions (DSC) further optimize memory by decomposing standard convolutions into smaller operations [79]. Detecting small water leakages in complex surroundings requires efficient feature extraction, and DSC helps reduce memory load while maintaining accuracy in resource-limited environment. Moreover, STDC2 further enhances memory efficiency by optimizing the backbone network, achieving robust feature extraction with substantially fewer parameters [22]. For efficient model updates and memory savings, SAM-Adapter introduces an adapter-based approach within Vision Transformer architectures. By inserting MLP layers at specific points in the network, only a small subset of parameters is uploaded, minimizing memory consumption during both training and inference [86].

Overall, efficiency-oriented methods play a pivotal role in advancing tunnel water leakage detection by enabling practical, real-time deployment in resource-constrained environments. These approaches emphasize optimization of inference speed and memory usage, addressing the critical need for fast and lightweight models in scenarios such as mobile inspections, embedded systems, and edge computing platforms. Through the adoption of lightweight network architectures, parameter pruning, depth wise separable convolutions, and memory-efficient frameworks, these methods significantly reduce computational load without compromising detection accuracy. Their contribution lies in achieving a balance between high-performance deep learning and real-world applicability, ensuring timely and scalable monitoring solutions for tunnel infrastructure maintenance.

5.2. Point cloud-based water leakage detection methods

While image-based methods have improved tunnel water leakage detection, they still suffer from notable limitations. Image quality is highly susceptible to environmental factors such as lighting conditions, environmental variability, and surface characteristics. These factors can introduce noise and distortions, leading to false positives or missed detections due to variations in surface color, texture, and reflection properties. LiDAR is unaffected by lighting conditions, making it a superior tool for the accurate and consistent detection of water leakage patterns in tunnels. Point cloud-based water leakage detection methods can be categorized as grid-based, voxel-based, and point-based. The general pipeline for each of these approaches is illustrated in Fig. 17. However, before implementing these methodologies, intensity correction of the point cloud data is essential. In LiDAR-based tunnel inspections, intensity correction plays a crucial role in ensuring the accuracy, consistency, and reliability of the extracted features. Uncorrected variations in sensor parameters, scanning angles, and surface reflectivity can distort intensity values and reduce the effectiveness of water leakage detection algorithms. This section first introduces key techniques for point cloud intensity correction, followed by an in-depth discussion of the three primary methodologies for water leakage detection.

5.2.1. Intensity correction

LiDAR systems emit laser beams and measuring the return time of echoes to measure the distance between the sensor and the target object while, generating point cloud data of the object's surface [87]. Since LiDAR sensors operate in the near-infrared spectrum, they are particularly effective for detecting water leakage on tunnel linings, even in low-light or complex environments. Different materials absorb or reflect near-infrared signals at varying levels, resulting in distinct point cloud intensity values. These intensity values correspond to the amplitude of the backscattered laser beam, providing valuable insights into the surface properties of the scanned object [88]. Water leakage areas on tunnel linings absorb more near-infrared radiation than dry surfaces, leading to lower intensity values in point clouds. By analyzing the spatial distribution of intensity values, water leakage can be effectively identified [37,89].

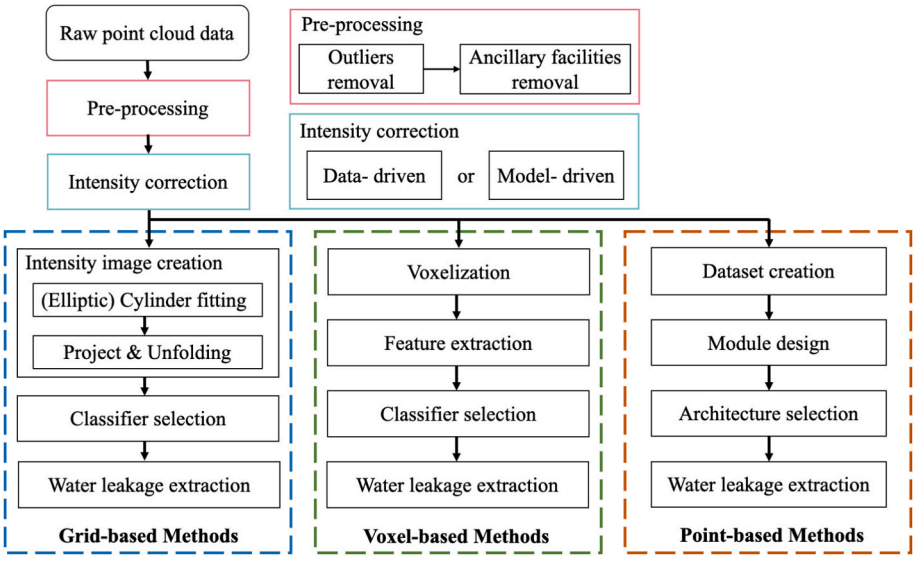

Fig. 17. General workflow of three common methods for water leakage detection.

Despite the advantages of intensity-based analysis, several challenges must be addressed before using raw LiDAR intensity data for water leakage detection. (1) Interference from ancillary tunnel structures. Ancillary structures (cable brackets, pipes, ventilation ducts) often yield low intensities due to their smooth metallic surfaces backscatter less energy, which can lead to false positives [39]. (2) Variation in distance and incidence angle. Accurately quantifying the variation of laser signals within a LiDAR scanner is inherently challenging, necessitating an intensity correction process that models the relationship between true intensity values and multiple influencing factors. These factors include the geometric relationship between the scanner and the target object, primarily the distance and laser incidence angle, as well as surface characteristics such as material composition, color, roughness, and moisture content. Among these, distance and incidence angle are the most critical parameters in intensity correction as they directly affect the strength of the reflected signal [90,91]. Sanchiz-Viel, et al. [88] conducted experiments using the Faro Focus 3D 120 LiDAR scanner to demonstrate how intensity values fluctuate with changes in distance and incidence angle, as illustrated in Fig. 18. The results include: (1) 0–6 m: Intensity fluctuations occur due to near-distance reducers preventing signal saturation. (2) 6–14 m: Intensity variations align with uncorrected signal measurements. (3) Beyond 14 m: The signal weakens significantly, requiring amplifiers to compensate. (4) Intensity values decrease nonlinearly as the incidence angle increases. Metro tunnel typically has radii of 2–5 m, laser beams rarely strike surfaces at a 0-degree incidence angle.

To minimize distortions and improve reliability, researchers have developed intensity correction models that account for distance, incidence angle, and surface characteristics. It is important to recognize that a generalized rule for the behavior of different LiDAR scanners cannot be established; instead, intensity correction models should be developed considering various influencing factors [92]. These models can be categorized as model-driven and data-driven methods [93].

Model-driven approaches are grounded in the assumption that laser signals emitted by the laser scanning system adhere to the radar equation (Eq. (1)). These approaches also presume that tunnel linings behave as Lambertian surfaces, which reflect light uniformly in all directions. Given these foundational assumptions, model-driven methods employ Eq. (2) [90] to correct the raw point cloud intensity, where ρ represents reflectivity, R denotes distance, and α indicates incidence angle. Model-driven approaches aim to standardize intensity measurements, enabling a more consistent interpretation of the point cloud data. However, assuming Lambertian reflectance overlooks non-uniform behavior of materials like segmented concrete linings, reducing model accuracy in practice.

$$\rho_L \propto \phi_r(\rho_L, R, \alpha)\frac{R^2}{\cos\alpha} \tag{1}$$

$$I_{cor}(\rho) = I_{raw}(\rho, R, \alpha)\frac{R^2}{\cos\alpha} \tag{2}$$

Data-driven methods use large-scale observational data instead of physical models for intensity correction. These methods apply pattern recognition to correct intensity values directly, reducing errors from incorrect model assumptions [94]. In tunnel environments, point cloud intensity is influenced by nonlinear interactions among factors such as distance, angle, material, and surface roughness. The correction process involves constructing models that predict point cloud intensity considering various influencing parameters, generating optimal correction coefficients. Table 2 summarizes several data-driven methods for point cloud intensity correction and the specific models employed [88]. These methods effectively minimize distortions in raw data by addressing the multifaceted factors impacting intensity values. As a result, intensity correction enhances the accuracy of water leakage detection by reducing the influence of ancillary structures and improving the identification of actual water leakage areas [95,96].

5.2.2. *Grid-based methods*

Tunnel inspections yield millions of 3D points per kilometer, each include spatial coordinates and intensity information. Processing such a massive amount of data requires substantial computational resources. The grid-based method reduces computational complexity by converting 3D point cloud data into 2D intensity images. The schematic diagram of this transformation is shown in Fig. 19. Specifically, algorithms such as Random sample consensus (RANSAC) are commonly used for fitting the tunnel point cloud data to cylindrical or ellipsoidal models. The point cloud is then projected onto the fitted surface and unfolded to form a 2D image, with intensity attributes assigned to each grid [102–106], as illustrated in Fig. 20. Recognizing the potential distortion introduced by standard projection techniques, particularly in cases of significant tunnel curvature, Chen, et al. [107] proposed a novel method utilizing cylindrical voxel structures to generate intensity images. This method

Table 2
Data-driven based point cloud intensity correction model. R[m]: distance, α[∘]: incidence angle, τ [dimensionless]: surface roughness, I_{raw}: raw intensity, I_{cor}: corrected intensity.

References	Variant	Equation	Scanner
Fang, et al. [97]	R, α	$I_{cor} = \frac{I_{raw}}{F_2(\alpha)F_3(R)}, F_2(\alpha) = h_\rho(1-n+n\cos\alpha)$	Faro Focus3D Z + F Imager5006i
Errington, et al. [98]	R, α	$I_{cor}(\rho_L, R, \alpha) = F(\rho_L, \alpha, G(R))$	Riegl VZ-400 Faro Focus 3D
Tan and Cheng [99]	R, α	$I_{cor}(\rho_L, R, \alpha) = I_{raw}(\rho_L)F_2(\cos\alpha)F_3(R)$	Faro Focus 3D X330
Xu, et al. [100]	R, α, τ	$I_{cor}(\rho_L, R, \alpha) = I_{raw}(\rho_L)F_2(\cos\alpha)F_3(R)$, $F_2(\alpha) = 10\log(\cos\alpha(A + B\sin\alpha\tan\alpha))$	Riegl VZ-400i
Bretagne, et al. [101]	R, α	$I_{cor}(R, \alpha) = \left[1805.4 - \frac{3075.8}{R}\right]\cos\alpha + 1473.9 - \frac{1510.5}{R} + I_{\min}$	Leica Scan Station C10

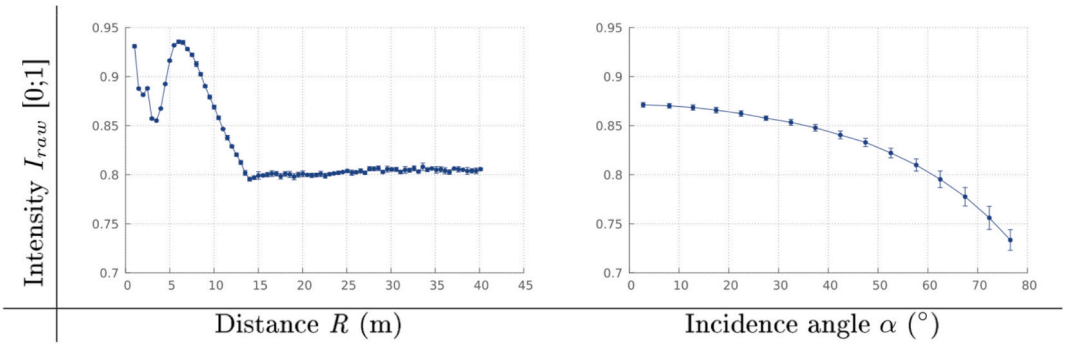

Fig. 18. Schematic of the relationship between raw intensity and distance, incidence angle [88].

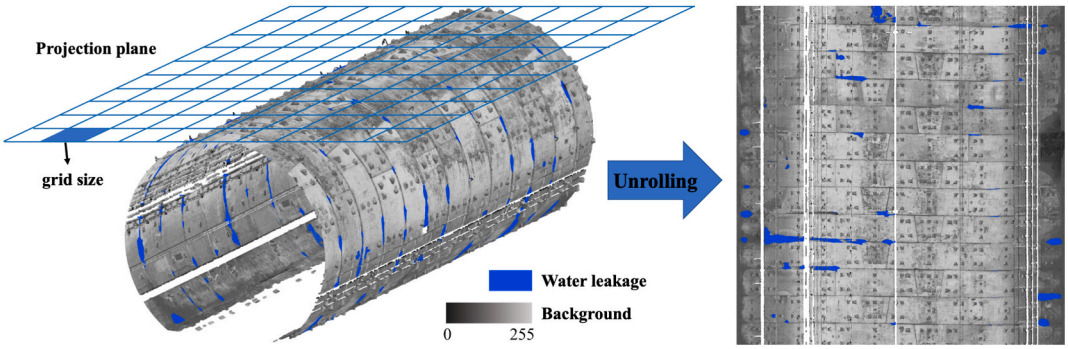

Fig. 19. The schematic of intensity image generation.

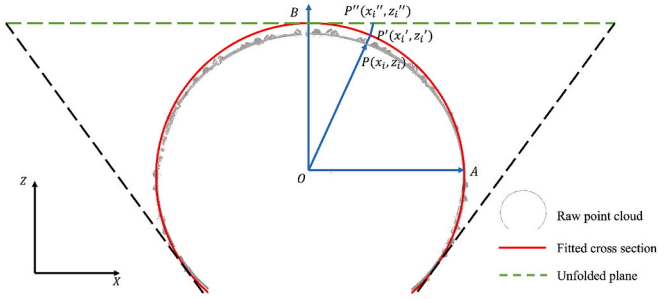

Fig. 20. Schematic of point cloud intensity map formed by projecting and unfolding the tunnel point cloud data.

divides the point cloud into cylindrical voxels and applies block-wise projection to preserve spatial structure and reduce distortion. However, converting 3D point cloud data into 2D images inevitably leads to information loss, particularly in terms of spatial structure and depth information. To address this, harmonic mapping can be employed to project complex 3D surfaces onto 2D planes while preserving essential information and topological features [108]. Notably, the selection of grid size is a critical process that significantly affects water leakage detection accuracy. An excessively large grid size (≫mean point spacing) smooths away intensity contrasts at water leakage edges, since leakage and non-leakage returns are aggregated within the same cell. Conversely, a grid size much smaller than the mean spacing produces empty cells, thereby degrading the continuity of the intensity map and reducing processing efficiency.

Given the intensity images, numerous researchers have conducted extensive studies on water leakage detection. Xu, et al. [95] proposed a threshold-based approach that defines potential water leakage with intensity values below the threshold of $\mu_I - 3\sigma_I$, where μ_I and σ_I denotes the mean and standard deviation of intensity, respectively. Additionally, Tan, et al. [89] derived a water content map by leveraging the linear relationship between the corrected intensity and moisture content based on the findings of Kaasalainen, et al. [109], Suchocki, et al. [110], and Suchocki, et al. [111]. The median filtering and defined threshold are further applied to remove bolt holes that were mistakenly detected as water leakages. However, the thresholds used in these methods are determined empirically, which limits their generalizability across different tunnel scenarios. In this context, machine learning techniques have emerged as a promising alternative. Traditional methods, such as region growing, connected component analysis, and edge detection algorithms, have gained prominence in image processing, showing the potential for application in water leakage detection [40].

Recently, deep learning has advanced image recognition and been applied to tunnel water leakage detection. Unlike conventional methods, convolutional neural networks (CNNs) excel by extracting complex representations from large datasets without manual feature selection. Mask R-CNN performs well in instance segmentation and is widely applied for tunnel water leakage detection [104,107,112,113]. Additionally, Cheng, et al. [114] proposed a modified FCN architecture, specifically designed to segment water leakage within the generated intensity images. Despite these advancements in water leakage detection, their limited receptive fields pose challenges in extracting multi-scale features. This limitation is particularly evident when dealing with water leakage regions of varying scales, where the networks may struggle to capture richer hierarchical features. To this end, researchers have developed a multi-scale deep feature network incorporating Res2Net modules to extract water leakage features [38]. Additionally, Zhang, et al. [115] developed a feature fusion model utilizing the Dempster-Shafer evidence theory to integrate local and global features from different CNN models. However, conventional convolutional operations may fall short in detecting heterogeneous water leakages due to their fixed receptive field and shared weight mechanism. To this end, attention mechanisms have been introduced for dynamic modulation of feature weights to focus on the most salient aspects of input data, while reducing the influence of irrelevant background elements. Zhang, et al. [106] enhanced U-Net with dual-attention modules to capture local details and global context concurrently. Additionally, Guo, et al. [103] advanced this approach by combing channel and coordinate attention to improve detection of horizontal and vertical water leakage patterns. Furthermore, deformable convolutions adapt kernels to varied water leakage shapes, enabling more precise detection of water leakage phenomena with diverse shapes and scales. However, the complexity of these deep learning models imposes significant computational and storage demands. These requirements present challenges for the efficient deployment of such models, particularly in resource-constrained environments. In response, Yin, et al. [105] employed the YOLOv5 network as backbone, optimizing its computational complexity for deployment on lightweight and portable devices.

To summarize, grid-based methods transform complex 3D point cloud data into more manageable 2D representations. This transformation simplifies data structure, reduces computational complexity, and enables the use of image-based analysis techniques. Therefore, these methods are particularly suitable for users with limited computational resources. These methods facilitate efficient data processing, support the deployment of automated detection algorithms, and enhance the scalability of inspection workflows. While grid-based approaches have demonstrated success cases in water leakage detection, their inherent limitations lay in the loss of spatial and geometric information during 2D grid projection. Another key challenge arises from the material properties of these auxiliary structures, which can produce point intensity similar to those of water leakages, leading to misclassification. Although intensity correction or structural filtering before rasterization can mitigate such interference, these preprocessing steps substantially increase computational overhead.

5.2.3. Voxel-based methods

Voxel-based methods form a fundamental approach in tunnel point cloud processing through voxel representation [116]. As illustrated in Fig. 21, this method transforms irregularly distributed tunnel point clouds into structured volumetric representations through spatial discretization into uniform cubic units. The voxelization process preserves original depth information and geometric relationships, facilitating precise spatial analysis and robust identification of water leakage regions. It is important to note that an appropriate voxel size is fundamental to balancing 3D detail preservation against computational and memory constraints in water leakage detection. In voxelization, a voxel size significantly larger than the average point spacing will blur intensity variations around water leakage sites, diminishing detection sensitivity. In contrast, a voxel size that is too small yields an increase of empty voxels, resulting in high memory consumption and longer runtimes.

Recent researches highlight the capabilities of voxel-based representations in detecting tunnel water leakage. Wang, et al. [7] leveraged voxelized data to develop an optimization framework combining k-nearest neighbors classification and Bayesian optimization. This voxel-based approach employs a Gaussian process to select hyperparameters automatically, improving accuracy and efficiency for complex water leakage patterns. In voxelization advancements, Wang, et al. [39] introduced a polar-voxel representation that preserves spatial information and improves water leakage detection accuracy. This strategy allows 3D connected-component analysis on voxel grids, mapping water leakage distributions for a comprehensive view of patterns. Moreover, Ji, et al. [117] developed an encoder-decoder architecture specifically designed for voxelized tunnel data. This framework exploits the regular structure of voxel grids to balance data compression with feature preservation, where the encoder extracts high-dimensional spatial patterns from voxels, and the decoder reconstructs detailed segmentation maps.

Overall, the intrinsic advantages of voxel-based methods become particularly evident when compared to 2D grid-based methods. Preserving 3D spatial relationships and geometric information enables precise water leakage localization through direct volumetric analysis. The capability to maintain geometric integrity supports the accurate assessment of complex water leakage patterns. This spatial understanding reveals critical spatial and geometric relationships often obscured in grid-based approaches, thereby providing a robust foundation for water leakage detection within shield tunnel scenarios. Therefore, these methods are particularly suited for applications requiring precise 3D localization of water leakage sites.

5.2.4. Point-based methods

Point-based approaches for tunnel water leakage detection directly process raw point cloud data without requiring conversion to representations like grids or voxels [37]. These methods preserve inherent spatial and geometric attributes at the point level, improving feature extraction for precise water leakage detection. This characteristic proves particularly valuable for detecting water leakage patterns that conventional grid-based methods might overlook, enhancing reliability and accuracy.

Unlike grid-based water leakage detection methods, point-based methods directly detect water leakages in 3D space and leverage geometric features to distinguish water leakages from auxiliary structures. Shield tunnels, constructed from prefabricated concrete segments (as shown in Fig. 22), are prone to longitudinal settlement, convergence deformation, and dislocations due to external stresses over time [118–120]. These deformations create pathways for groundwater infiltration through segment joints, grouting holes, and bolt holes, resulting in water leakage predominantly at these areas, as shown in Fig. 23(d). Notably, these areas exhibit distinct geometric features compared to the tunnel lining surface. To visualize these distinctions, the Fast Point Feature Histogram (FPFH) algorithm [121] was employed to extract geometric descriptors from tunnel point cloud data. The computational workflow (Fig. 23(b), [122]) generates per-point histograms encoding surface curvature variations and neighborhood relations. As visualized in Fig. 23(c), areas such as bolt holes, circumferential joints, grouting holes, and longitudinal joints display unique geometric signatures, distinguishing them from the tunnel lining surface. This phenomenon corroborates the conclusions drawn by Yin, et al. [105] and Yu, et al. [123]. These findings highlight the limitations of grid-based approaches in fully capturing the geometric information in 3D point cloud data for water leakage detection. Even voxel representations result in information loss, particularly when detecting fine-scale water leakages. Recent advancements in point-based methods demonstrate enhanced performance through leveraging latent inter-point relationships [124,125].

In conclusion, point-based methods offer an alternative for tunnel water leakage detection by directly operating on raw point cloud data, thus preserving complete spatial and geometric information. Point-based strategies maintain the integrity of 3D structures and enable

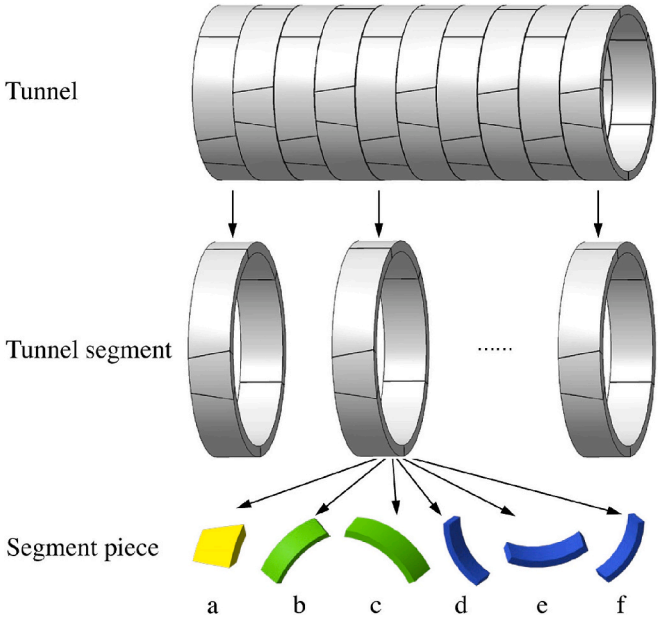

Fig. 22. Illustration of the hierarchical structure of the tunnel [126].

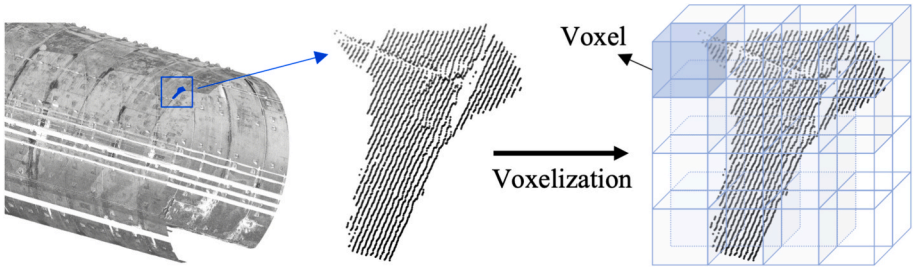

Fig. 21. Schematic of point cloud voxelization.

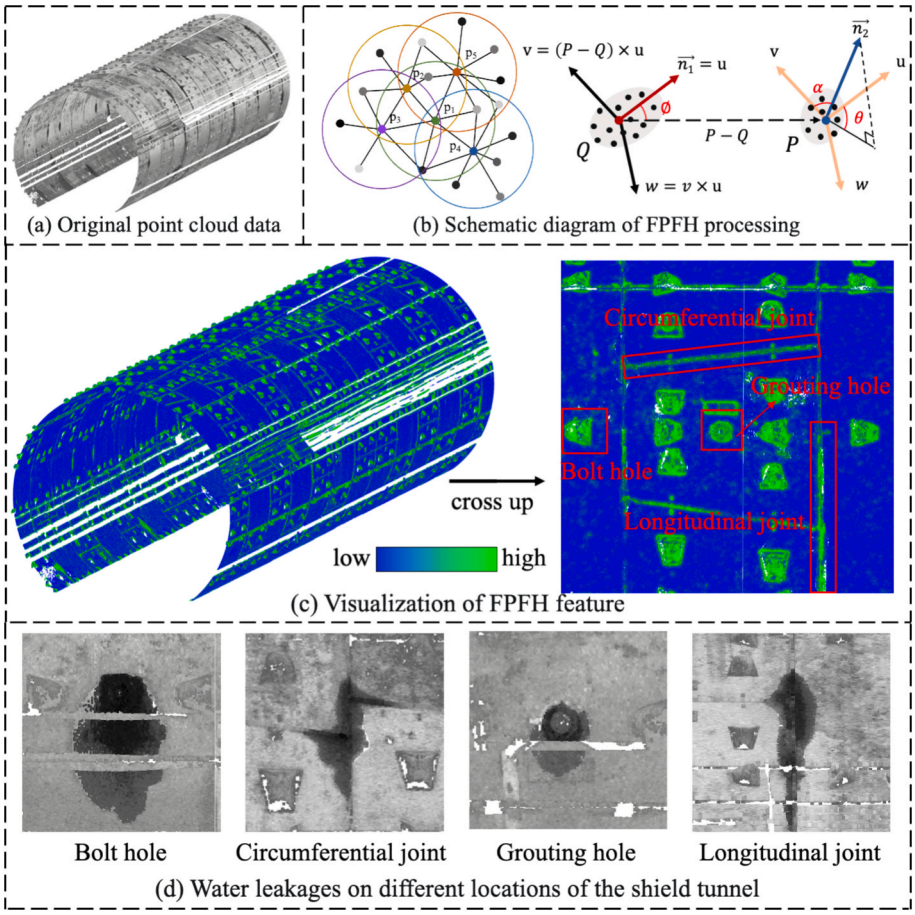

Fig. 23. The spatial characteristics of the location of tunnel water leakage.

more precise differentiation between water leakage areas and surrounding tunnel features. This capability is especially important for identifying subtle water leakages that coincide with structural deformations or occur near complex geometries. Therefore, these methods are applicable when precise 3D localization of water leakage sites and accurate estimation of water leakage area are required. While still relatively underexplored, point-based methods demonstrate strong potential for improving detection accuracy and reliability. Their ability to retain fine-scale spatial characteristics makes them a promising direction for future research in automated tunnel inspection and defect analysis.

5.3. *Infrared thermal-based water leakage detection methods*

5.3.1. *Basic principles*

Infrared thermal sensors detect infrared radiation emitted by objects. These sensors capture infrared radiation and convert it into thermal images, facilitating the visualization of temperature distributions across surfaces [127]. This non-contact temperature mapping reveals underlying conditions that are not discernible through conventional visual inspection. In water leakage detection, the presence of water alters the thermal conductivity of tunnel lining materials, leading to localized temperature anomalies. Specifically, water leakage typically results in cooler areas on the thermal image, as water reduces the surface temperature. Han, et al. [42] employed an image processing algorithm to extract temperature values along a designated pixel line (Line 1) in an infrared image. The temperature within the water leakage area (between points A and B) was significantly lower than that of the surrounding tunnel surface, as shown in Fig. 24. Detecting these temperature anomalies is essential for accurately identifying water leakage locations.

5.3.2. *Detection methods*

Inagaki and Okamoto [127] pioneered the use of infrared

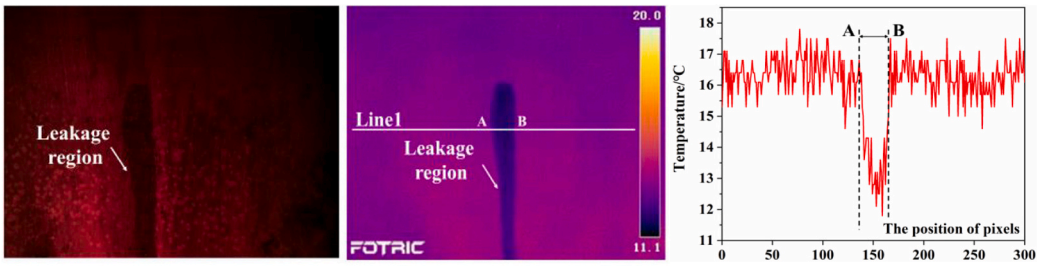

Fig. 24. Water leakage region representation difference between RGB and IR image [42].

thermography for detecting water leakage on structural surfaces. Their seminal work demonstrated the feasibility of thermal imaging in identifying temperature anomalies associated with water leakage. Recent studies have incorporated advanced techniques to enhance the accuracy and efficiency of water leakage detection using infrared thermography. Lu, et al. [45] developed an automatic inspection system for tunnels that integrates infrared thermography with image processing algorithms. This system captures infrared images of tunnel lining surfaces and applies grayscale conversion, noise filtering, binarization, and threshold segmentation, to identify potential water leakage regions. Further advancement is the application of multitemporal infrared thermography, as demonstrated by Yahia, et al. [128]. This method distinguishes persistent temperature variations indicative of water leakage from transient thermal anomalies. Despite these advancements, traditional infrared thermography methods typically depend on predefined algorithms and manual feature extraction. This reliance restricts their adaptability to the diverse and complex conditions encountered in practice. To this end, deep learning has emerged as a robust alternative. Luo, et al. [12] proposed a deep learning framework that employs VGG-U Net and LSTM networks for spatial segmentation and temporal analysis, mitigating the limitations of conventional methods. The inclusion of a cross-network learning strategy further improves detection accuracy and robustness.

However, the low resolution of thermal images often fails to capture the fine details necessary for precise water leakage detection. Additionally, thermal images also suffer from noise and environmental effects such as temperature and humidity changes, which may lead to error detection. To address these limitations, recent research has focused on integrating infrared thermal sensors with complementary sensors, including RGB cameras and LiDAR systems. Yu, et al. [123] developed a novel system that combines laser scanning with infrared thermal imaging for diagnosing water leakage. This method initiates with laser scanning to generate a point cloud, from which potential water leakage areas are identified by intensity values. Subsequent refinement using thermal images filters out false positives while supplying critical temperature-based information. Similarly, Han, et al. [42] proposed a one-stage anchor-free multispectral modality fusion network that integrates visual-optical (VIS) and thermal infrared (IR) sensor data. Their CNN architecture effectively merges features from both VIS and IR images, thereby mitigating the limitations inherent in each modality.

Overall, infrared thermal-based methods offer a non-contact and efficient approach to tunnel water leakage detection by capturing temperature anomalies caused by water leakage. Their ability to operate in low-light environments and rapidly scan large areas makes them well-suited for tunnel inspection. The integration of machine learning and deep learning techniques has significantly improved the interpretation of thermal data. Moreover, combining thermal imaging with complementary sensing techniques addresses the limitations of low resolution and environmental sensitivity, enabling more robust and comprehensive detection systems.

5.4. Conclusion

As summarized in Table 3, photogrammetry-based approaches leverage low-cost RGB imagery to enable fast, lightweight inspections with low computational requirements. This makes them ideal for preliminary assessments and resource-constrained scenarios. However, they lack of 3D context and sensitivity to lighting limit their precision. Grid-based LiDAR methods transform complex 3D point clouds into 2D intensity maps, achieving efficient large-scale processing and robustness to illumination changes. However, they may lose geometric detail and are sensitive to grid size. Voxel-based techniques preserve volumetric structure and depth information, enabling precise 3D water leakage localization, although they demand greater memory and processing overhead and may suffer from sparse zone errors. Point-based algorithms operate directly on raw point clouds to maintain complete spatial and geometric detail, offering the higher accuracy and the ability to delineate subtle water leakage features near complex geometries.

Table 3
Summary of different water leakage detection methods.

Sensors	Method type	Detection cue	Advantages	Limitations
Photogrammetry	Efficiency-oriented	RGB	1. Fast processing; 2. Low cost; 3. Easy deployment; 4. Lightweight.	1. Limited accuracy; 2. Lighting sensitive; 3. Water-glare interference; 4. Sensitive to image noise; 5.Lack of spatial information;
	Accuracy-oriented	RGB	1. High detection accuracy; 2. Fine detail segmentation; 3. Automatic feature learning; 4. Strong robustness.	1. Slow processing; 2. Lighting sensitive; 3. Water-glare interference; 4. Sensitive to image noise; 5. Lack of spatial information.
LiDAR	Grid based	Point intensity	1. Efficient large-scale data processing; 2. Robust to lighting variation; 3. Fast running time.	1. Grid size limitation; 2. Lack of spatial information; 3. Limited accuracy; 4. Additional storage require; 5. Non-end-to-end.
	Voxel based	Point intensity + Geometric feature	1. Robust to lighting variation; 2. High 3D spatial precision; 3. Flexible end-to-end learning; 4. Noise robust.	1. High computational complexity 2. Errors in sparse zones; 3. High memory demand;
	Point based	Point intensity + Geometric feature	1. Geometry preserved; 2. High 3D spatial precision; 3. Flexible end-to-end learning; 4. High detection accuracy.	1. Difficulty in balancing accuracy and efficiency; 2. Complex network design; 3. High memory demand; 4. Large labeling workload.
Thermal infrared	Unimodal based	Temperature	1. Real-time inspection; 2. Reveals hidden leakage.	1. Ambient temperature influence; 2. Low spatial resolution; 3. Affected by surface materials.
	Multi-modal based	Temperature + RGB/Point intensity/Geometric feature	1. Complementary information; 2. Enhanced robustness; 3. High detection accuracy.	1. Complex sensor calibration 2. Costly fusion algorithms; 3. Higher hardware expense

However, they require sophisticated network architectures and extensive labeling effort. Thermal infrared methods enable real-time anomaly detection and can uncover hidden water leakages. However, they suffer from low spatial resolution and are affected by ambient temperature. Multimodal fusion strategies combine thermal, RGB, or LiDAR data to enhance robustness and detection performance, but they introduce additional sensor-calibration complexity, higher hardware costs, and more elaborate data-fusion algorithms.

6. Discussion and outlook

6.1. Performance evaluation metrics

Primary evaluation metrics for tunnel water leakage detection include Precision, Recall, Accuracy, Intersection over Union (IoU), Average Precision (AP), F1-score, and Error Rate (Eqs. (3)–(9)). Notably, some studies evaluate overall algorithm performance across multiple defect types rather than water leakage. In such cases, mean metric values are employed to provide an assessment of the algorithm's performance.

$$\text{Precision} = \frac{TP}{TP + FP} \tag{3}$$

$$\text{Recall} = \frac{TP}{TP + FN} \tag{4}$$

$$\text{Accuracy} = \frac{TP + TN}{TP + TN + FP + FN} \tag{5}$$

$$\text{IoU} = \frac{TP}{TP + FP + FN} \tag{6}$$

$$\text{AP} = \sum_{n} (R_n - R_{n-1}) P_n \tag{7}$$

$$\text{F1 - score} = 2 \times \frac{\text{Precision} \times \text{Recall}}{\text{Precision} + \text{Recall}} \tag{8}$$

$$\text{Error rate} = \frac{FP + FN}{TN + TP + FN + FP} \tag{9}$$

where TP (True Positive) represents the correctly identified water leakage, FP (False Positive) denotes the non-leakage incorrectly identified as water leakage, FN (False Negative) is actual water leakage that were not detected, and TN (True Negative) corresponds to the correctly identified non-leakage. R_n and P_n are the recall and precision values, respectively. Precision measures the proportion of correctly identified water leakage instances among those predicted, while Recall assesses the proportion of actual leakage instances detected. Accuracy provides an aggregate measure of correctness for both leakage and non-leakage instances. The IoU quantifies the spatial overlap between predicted regions and the ground truth. The F1-score, as the harmonic mean of Precision and Recall, balances these two measures. AP summarizes performance across various thresholds as the area under the Precision-Recall curve, while the Error Rate represents the proportion of incorrect predictions relative to the total number of samples. In addition, efficiency metrics including Frames Per Second (FPS, quantifies processing speed), Giga Floating Point Operations per Second (GFLOPs, measure computational complexity) are used. Moreover, inference time evaluates how quickly the model generates results, and the number of parameters provides insights into model complexity and resource requirements, while model storage size determines memory consumption.

6.2. Qualitative analysis of approaches

6.2.1. Photogrammetry-based methods

Table 5 summarizes various accuracy-oriented techniques, highlighting their performance and the specific modules designed to enhance accuracy. However, due to the absence of a standardized dataset and evaluation metrics across these methods, direct cross-comparison is not feasible. Consequently, the quantitative assessments presented are constrained to demonstrating improvements within each approach.

The improvements in these methods primarily encompass four aspects: sample augmentation, feature enhancement, loss functions, and post-processing. (1) Sample augmentation enhances model robustness and generalization. Transfer learning further facilitates domain adaptation by initializing networks with pre-trained weights from large-scale datasets such as COCO [70,74] and PASCAL VOC2012 [129]. However, the gap between generic pre-training data and tunnel water leakage patterns requires developing domain-specific pre-training datasets. Additionally, the manual annotation of water leakage data remains labor-intensive. A promising alternative is weakly supervised learning, where pseudo-labels are generated using techniques like Class Activation Mapping (CAM) [80]. (2) Feature fusion techniques, such as skip-connections [67,75] and path aggregation modules [79], integrate multi-scale information to capture both global and local water leakage features. Advanced feature extraction architectures, such as FPN and EfficientNet, further enhance detection accuracy by extracting high-quality features across multiple resolutions. Additionally, attention mechanisms further refine feature selection by emphasizing water leakage areas, while suppressing background noise. Future research should focus on context-aware attention modules specifically optimized for heterogeneous water leakage patterns. (3) To mitigate sample imbalance, reweighted loss formulations such as Focal Loss [75,80] or Dice Loss [67] strategically emphasize positive samples while suppressing negative classes through adaptive weighting. Future research may explore novel loss functions to further optimize the trade-off between precision and recall, particularly for detecting small-scale tunnel water leakages. (4) Post-processing techniques refine water leakage predictions by applying image processing algorithms to eliminate false positives and enhance boundary precision in segmentation masks [17,74]. While effective, such post process approaches lack end-to-end trainability, limiting their adaptability in real-time systems. A promising alternative involves cascaded networks where a coarse detection stage guides refinement subnets to boost accuracy while preserving efficiency. Collectively, the integration of these modules substantially improves the accuracy of water leakage detection, with most algorithms achieving over 80 % precision, as shown in Table 5. However, tunnels are inherently complex 3D structures where adjacent elements often share similar textures or colors with water leakages. The inherent limitation of RGB images restricts the ability to accurately differentiate between these elements and water leakage. Future research should incorporate additional modalities, such as depth information, to improve the differentiation between water leakage and other tunnel components. Additionally, the similarity in texture and color between water leakage edges and the surrounding tunnel lining complicates precise edge detection, which is critical for analyzing water leakage propagation. Consequently, future efforts should develop edge delineation techniques to facilitate the analysis of water leakage diffusion pathways.

Table 4 summarizes key efficiency-oriented methods and their contributions to efficiency optimization. For inference speed, several fast backbone networks, such as YOLO [48] and ShuffleNet [75], have been employed to expedite detection. Additionally, modules like Depthwise Separable Convolution [79] reduce complexity by factorizing standard convolutions, resulting in improvements in FPS. Adaptive techniques such as Adaptive Order ROI [81] allow networks dynamically adjust processing strategies to reduce inference time. However, balancing memory usage with detection accuracy remains challenging. Larger models with more parameters can capture finer details of water leakages but require substantial memory resources. Future research should explore lightweight architectures that maintain high detection accuracy

Table 4
Shield tunnel water leakage detection using Photogrammetry-based methods (Efficiency-oriented). DL: Deep learning, Param.: Parameters of model (Million), MS: Model storage space.

Source	Method type	Backbone/ raw model	Improvement	Inference speed (raw model)	Memory usage (raw model)
Tan, et al. [75]	DL	ShuffleNet v2	TensorRT	FPS: 123.68 (68.41)	Param.: 10.2 M (5.9 M)
Zhou, et al. [79]	DL	YOLOv4	Depthwise separable convolution	FPS: 43.5 (32.9)	MS: 49.3 MB (250.6 MB)
Feng, et al. [67]	DL	U-Net/ U-Net++	EfficientNet, Bottleneck residual block	GFLOPs: 2164.5 (3435.7)	Param.: 30.0 M (29.24 M)
Chen, et al. [48]	DL	YOLO-V7	Non-maximum suppression	Infer time: 37.8 ms (39.0 ms)	Param.: 37.87 M
Gao, et al. [81]	DL	FCN	Adaptive order ROI	Infer time: 1.13 s (3.71 s)	NA
Wang, et al. [71]	DL	U-Net	EfficientNet-B0, scSE	FPS: 90	Param.: 5.1 M

while reducing memory requirements, potentially through network pruning or model quantization.

6.2.2. Point cloud-based methods

Table 6 presents a comparative analysis of these approaches, highlighting that voxel-based and point-based methods achieve higher accuracy than grid-based methods. This discrepancy primarily stems from the geometric sensitivity required for water leakage detection, where water leakages predominantly localize around segment joints, bolt holes, and grouting holes. These regions exhibit distinct geometric features that are better preserved by voxel-based and point-based methods, allowing for more effective detection. In contrast, grid-based methods convert 3D data into a 2D representation, leading to the loss of essential geometric and spatial information. This dimensional reduction limits the capacity to capture the geometric complexity of water leakage regions, resulting in degraded detection performance.

Despite advancements in point cloud-based methods, various researches still convert point cloud data into 2D representations, utilizing image processing techniques for water leakage detection. This preference arises from several intrinsic challenges associated with point cloud data: (1) Data characteristics. Unlike image data, where pixels are arranged in a structured grid, point cloud data is inherently unordered, sparse, and irregular, posing significant challenges for algorithm design. The absence of explicit neighborhood connectivity necessitates specialized architectures to infer implicit spatial relationships, significantly increasing algorithmic design complexity. (2) Computational complexity. Unlike 2D images, point clouds encode 3D spatial information, increasing both computational resource requirements and processing complexity. High-resolution tunnel scans generate dense point clouds with 3D coordinates, rendering real-time processing computationally expensive and limiting the feasibility of point cloud-based approaches for practical water leakage detection. (3) Maturity of image-based technologies. Deep learning for image-based tasks has undergone substantial advancements, leading to the development of well-established neural network architectures for segmentation, detection, and classification. These mature models can be directly applied or adapted with modifications when point cloud data is projected onto a 2D plane. This renders the preference for grid-based approaches in water leakage detection. Despite the challenges associated with implementing point-based and voxel-based methods, processing 3D data remains essential. This necessity stems from both the distinct geometric characteristics of water leakage areas and the complexities of tunnel environments, where auxiliary structures often exhibit similar intensity values to water leakage regions in point cloud data, as analyzed in Section 5.2.

To address these challenges, several practical solutions can be implemented. One promising approach involves employing multi-resolution representations through hierarchical data structures such as Octrees or KD-trees. These structures enable progressive data refinement during processing, which reduces computational load by initially processing the data at a coarse resolution and subsequently refining analysis in water leakage regions [131]. Moreover, sparse tensor representations store and process only the non-empty regions of the point cloud, further reducing computational costs, as demonstrated by techniques such as Sparse Convolution [132] and OA-CNNs [133]. Additionally, given the computational demands of training deep learning models on large-scale point cloud datasets, transfer learning offers an effective strategy. Models trained on large-scale 3D datasets for tasks such as object detection or scene understanding can serve as a foundation for fine-tuning on tunnel water leakage detection tasks. Alternatively, geometric feature–based filtering offers an effective approach. Principal Component Analysis and normal vector estimation isolate planar surfaces, edges, and curvature, which are the key characteristics of auxiliary tunnel elements such as bolts and cables. Local geometric descriptors, including Point Feature Histograms (PFH) [134], Fast Point Feature Histograms (FPFH) [121], and Signatures of Histograms of Orientations (SHOT) [135], capture the finer geometric properties of point-cloud regions. By integrating these features, models can distinguish water leakage from areas with similar intensity values, enhancing detection accuracy and reducing false positives.

Additionally, as demonstrated in Table 6, deep learning methods consistently outperform machine learning approaches. This superiority stems from the ability of deep learning models to automatically learn and extract complex features from large datasets, while machine learning methods rely on manually designed features that may not fully capture the intricacies of tunnel water leakage patterns. Deep learning-based methods are generally enhanced through several mechanisms. (1) Feature perception enhancement. A major advantage of deep learning lies in its ability to encode both local and global features through hierarchical feature extraction. Local feature encoding captures fine-grained details essential for identifying small-scale water leakages, while global feature encoding provides broader contextual information to distinguish water leakage regions from surrounding tunnel structures. (2) Multi-scale feature fusion. Integrating multi-scale features enables deep learning models to effectively process water leakages of varying sizes. Techniques such as the Bidirectional Feature Pyramid Network (BiFPN) facilitate feature fusion across multiple scales, improving the detection of both large structural patterns and small localized defects [105]. (3) Attention mechanisms play an increasingly important role in deep learning models by selectively focusing on relevant regions of the input data. In water leakage detection, these mechanisms assign dynamic weights to suppress background noise and auxiliary structures with leakage-like point-cloud intensities, thereby isolating water leakage regions [103,106]. (4) Adaptive convolutional operations further improve model adaptability by dynamically adjusting to local geometric variations, such as Edge Convolution [115] and Deformable Convolution [103]. Tunnel environments often contain structural elements such as bolts, cables, and grout holes, which introduce irregularities in surface geometry. Standard convolutional operations may struggle to accurately model these geometric differences. In contrast, geometrically adaptive convolutions improve the model's ability to capture fine-grained spatial variations, enhancing detection accuracy in complex tunnel conditions.

Despite the significant advantages of deep learning methods, several challenges persist in tunnel water leakage detection. (1) Sample imbalance. Water leakage instances typically represent a small proportion of the dataset compared to non-leakage areas, leading to a bias

Table 5
Shield tunnel water leakage detection using Photogrammetry-based methods (Accuracy-oriented). DL: Deep learning, ML: Machine learning, Acc: Accuracy, IoU: Intersection over Union, AP: Average Precision, Pre: Precision, Rec: Recall, F1: F1 score, ER: Error rate, NA – Not available. Note: The *underlined and italicized front* indicates the metric value of water leakage categories, and the normal font represents the average of all categories. Unit: %.

Source	Method type	Backbone	Sample augmentation	Feature enhancement	Loss function	Post-processing	Acc	IoU	AP	Pre	Rec	F1	ER
Xue and Li [19]	DL	FCN	Data augmentation	Position-sensitive RoI pooling	Softmax and bounding box regression	NA	95.84	/	/	93.80	87.40	/	/
Tan, et al. [75]	DL	ShuffleNet v2	Data augmentation	Skip-connection	Focal loss	NA	97.38	81.67	88.61	/	/	/	/
Xu, et al. [74]	DL	Mask RCNN	Transfer learning	Path augmentation feature pyramid	Multi-task loss	Edge detection	/	/	95.35	/	/	/	0.61
Li, et al. [18]	DL	Faster R-CNN	Data augmentation	Multi-layer Feature fusion, Anchor enhancement	Focal loss	NA	/	/	88.50	*94.60*	97.00	/	/
Zhou, et al. [79]	DL	YOLOv4	Mosaic data augmentation	EfficientNet, Path aggregation	Multi-task loss	NA	/	/	*82.31*	/	/	*82.14*	/
Huang, et al. [17]	DL	FCN	Label-preserving transformations	NA	Cross entropy loss	Dilation, Erosion	/	/	/	/	/	/	1.1
Feng, et al. [67]	DL	UNet++/ UNet	Data augmentation	EfficientNet, Skip connection	Dice loss	NA	/	87.8	/	/	/	/	/
Xue, et al. [47]	DL	Mask RCNN	Data augmentation, Transfer learning	Cascade, Feature pyramid network	Multi-task loss	NA	/	/	51.1	/	/	/	/
Qiu, et al. [80]	DL	DeepLabV3+	Adaptive pixel segmentation clustering	Res2Net, Channel/ spatial attention	Focal loss	NA	/	82.8	/	80.6	85.2	82.9	/
Xu, et al. [23]	DL	ResNet-101	Data augmentation	Pyramid pooling module, Expanded threshold search	Focal loss Lovasz-softmax loss	NA	/	*65.6*	/	/	*89.86*	*89.86*	*3.93*
Qin, et al. [130]	DL	ViT	NA	Convolution prior module; feature injector module	NA	NA	93.77	88.36	/	/	/	92.93	/
Tan, et al. [22]	DL	STDC2	NA	Convolutional block attention, CoT contextual transformer	Binary cross-entropy loss	NA	/	*88.18*	/	*91.93*	*95.58*	*93.72*	/
Dawood, et al. [58]	ML	Canny edge detection, Image processing (dilation and erosion)					/	/	/	96.1	93.2	/	/

Table 6
Shield tunnel water leakage detection using Point cloud-based methods. DL – Deep learning, ML –Machine learning, AP – Average Precision, AP50/75 – Average Precision at IoU = 0.5/0.75, Pre – Precision, Rec – Recall, F1 – F1 score, IoU – Intersection over Union, NA – Not available. Note: The "m" before the metric indicates the average value of the metric across different categories. Accuracy metrics unit: %.

Source	System	Data processing type	Method type	Raw model/ Backbone	Efficiency	Accuracy	Improvement	Accuracy
Liu, et al. [38]	MLS	Gird	DL	Res2Net	0.20 (s per image)	AP: 57.2 AP50: 82.2 AP75: 65.1	Cascade	AP: 60.0 AP50: 85.8 AP75: 68.2
Ji, et al. [117]	MLS	Voxel	DL	3D CNNs	NA	NA	Feature fusion, Normalization	Pre: 90.12 Rec: 77.43 F1: 83.29 IoU: 71.37
Yin, et al. [105]	MLS	Grid	DL	YOLOv5	NA	NA	Bidirectional feature pyramid network	Pre: 82.1 Rec: 63.2 F1: 71.4
Zhang, et al. [115]	MLS	Grid	DL	DGCNN	NA	IoU: 54.5 Rec: 89.1 Pre: 58.4 F1: 70.1	Edge convolution, Dempster-shafer evidence feature augment	IoU: 70.0 Rec: 89.6 Pre: 76.2 F1: 82.4
Guo, et al. [103]	MLS	Grid	DL	YOLOv5	NA	Pre: 81.1 Rec: 73.5 F1: 77.1 mAP: 58.8	Deformable convolution, Attention mechanism, Soft-NMS	Pre: 81.6 Rec: 77.1 F1: 79.3 mAP: 64.0
Li, et al. [124]	MLS	Point	DL	NA	514.52 (FLOPs)	NA	Global and local feature encoding, Local feature discriminative aggregation	mIoU: 73.2
Zhang, et al. [106]	MLS	Grid	DL	U-Net	0.0124 (s/1e6 points)	IoU: 60.0 Rec: 69.8 Pre: 81.0 F1: 75.0	Attention mechanism, Weighted Loss	IoU: 66.0 Rec: 86.4 Pre: 73.6 F1: 79.5
Chen, et al. [107]	TLS + MLS	Grid	DL	Mask RCNN	0.0017 (s per image)	NA	Cylindrical Voxel	mPA: 92.0 mIoU: 87.5
Liu, et al. [136]	MLS	Grid	DL	NA	28.6 (GFLOs)	mAP: 57.4	Receptive field expansion convolution; Attention-inducing downsampling unit	mAP: 66.2
Zheng, et al. [137]	MLS	Grid	DL	YOLOv8	10.7 (ms per image)	AP: 82.9	Coordinate attention; Bottleneck Transformer	AP: 92.3
Wang, et al. [138]	MLS	Point	ML	3D OTSU	NA	Pre: 46.8 Rec: 85.0 F1: 60.4	KNN, Delaunay boundary distance threshold.	Pre: 48.8 Rec: 85.0 F1: 62.0
Wang, et al. [7]	TLS	Point	ML	Naïve Bayes	NA	Pre: 31.8 Rec: 78.3 F1: 45.2	Gaussian process, Bayesian optimized KNN	Pre:54.3 Rec: 95.9 F1: 69.3
Wang, et al. [39]	MLS	Voxel	ML	Spatially Connected Component	NA	NA	NA	Rec: 93.15
Li, et al. [37]	TLS	Point	ML	Threshold	0.3 ~ 0.5 (h per scene)	NA	NA	Pre: 92.0

toward the majority class. This imbalance hinders the model's effective learning of the distinctive features of tunnel water leakage. To mitigate this issue, future work should explore data augmentation techniques, such as geometric transformations or synthetic data generation, to artificially increase the number of water leakage samples. Additionally, weighted loss functions that impose greater penalties on misclassified minority samples, including Focal Loss and Dice Loss, enable the model to focus on underrepresented water leakage cases. (2) Limited generalization capability. Deep learning models often struggle to maintain high performance when applied to unseen data, as variations in tunnel environments, scanning conditions, and sensor noise can significantly affect model robustness. This limitation restricts the practical applicability of these models across diverse real-world scenarios. To improve generalization, future research should investigate domain adaptation techniques and transfer learning strategies. Moreover, assembling large-scale, diverse datasets for training and validation can expose models to a wider range of conditions. (3) Challenges in capturing global features. The unordered and irregular nature of point clouds complicate the capture of global contextual information, which is essential for understanding water leakage patterns that span extensive regions. Future efforts may benefit from developing advanced neural network architectures to better capture both local and global spatial relationships, such as graph neural networks or transformer-based models.

6.2.3. *Infrared thermal-based methods*

The application of infrared thermal imaging in tunnel water leakage detection remains underexplored. Most existing research integrates infrared thermal sensors with other sensors, such as RGB cameras [42] or laser scanning [123]. The scarcity of dedicated studies hinders the comprehensive evaluation of infrared thermal-based methods. However, infrared thermal imaging offers valuable insights into subsurface conditions that may not be detectable through visual inspection or conventional imaging methods. However, several factors constrain its widespread adoption and effectiveness in tunnel water leakage detection. The thermal conditions within tunnels are inherently complex and affected by factors such as external temperature fluctuations and heat sources from equipment or vehicles. These factors can mask or distort the thermal signatures of water leakage, making it challenging to distinguish water leakages from background thermal noise. Moreover, the dynamic tunnel environments complicates consistent data

acquisition. The advancement of infrared thermal-based methods also stems from poor resolution and high sensitivity. Infrared cameras typically have lower spatial resolution than RGB cameras, limiting their ability to detect small-scale water leakages. Infrared sensors may also lack the sensitivity required to capture subtle temperature differences caused by water leakage, especially in low thermal contrast conditions. Additionally, the interpretation of thermal images requires expertise to accurately classify temperature anomalies. The absence of standardized protocols for thermal data analysis in tunnel environments contributes to inconsistencies in both research and application.

Future research could focus on several aspects, including advanced data processing techniques, sensor technique improvements, and multimodal data fusion strategies. Employing advanced image processing and machine learning algorithms tailored for thermal data can enhance the extraction of meaningful features. Deep learning, thermal image segmentation and pattern recognition, shows great promise in enhancing detection capabilities. In parallel, further developments in infrared sensor technique are critical. Sensors with higher spatial resolution, greater thermal sensitivity, and enhanced durability for tunnel environments are required. Additionally, multimodal data fusion presents a promising technique for improving the robustness and accuracy of water leakage detection. The development of effective data fusion algorithms, including sensor alignment, feature-level fusion, and deep multimodal learning models, are essential to seamlessly integrate these modalities and enhance overall system performance.

6.3. Future work

Currently, the primary sensing systems utilized for shield-tunnel water leakage detection include photogrammetry, laser scanning, and infrared thermal imaging, each demonstrating unique advantages alongside notable limitations. Recently, some research has begun developing multi-sensor scanning platforms for shield tunnel inspection. However, these integrated multi-sensor systems are still at an early stage of development. Future studies should prioritize the advancement of comprehensive multi-sensor platforms designed specifically for detecting multiple defect types in shield tunnels simultaneously. Furthermore, although several recent studies have employed multiple sensing modalities, current approaches typically process data from different sensors independently, thereby not fully exploiting the complementary nature of multimodal data. Consequently, future research should not only develop multi-sensor scanning systems but also corresponding multimodal data fusion algorithms to effectively integrate different sensing data streams, thus achieving enhanced detection accuracy and reliability.

In addition, recent trends increasingly emphasize lightweight methodologies to facilitate deployment under resource-constrained conditions and to enable real-time monitoring. This shift highlights the growing practical importance of efficiency and real-time operation in actual engineering applications. To practically implement lightweight methodologies, several promising approaches can be explored in future research. One direction involves model compression techniques, such as model pruning, and knowledge distillation. These methods aim to reduce model parameters and computational complexity while maintaining acceptable accuracy. Another potential solution is architecture optimization, including the development of efficient neural network structures tailored specifically for point cloud data, such as lightweight convolutional neural networks. Moreover, incorporating depth-wise separable convolutions and simplified attention mechanisms can further enhance computational efficiency. Finally, integrating edge computing and incremental learning strategies could significantly improve the feasibility of real-time and resource-efficient deployment in shield-tunnel water leakage detection. Nevertheless, achieving an optimal balance between algorithmic accuracy and computational efficiency remains a challenging task, especially for methods utilizing deep learning techniques or operating on extensive point-cloud datasets. Therefore, future investigations need to specifically focus on methods capable of effectively balancing accuracy and computational efficiency, thereby enhancing the practical applicability and real-world feasibility of shield-tunnel water leakage detection systems.

Moreover, existing detection algorithms often achieve high performance only within their respective training datasets. However, their robustness and generalization capability remain relatively untested. The variability in data collected by different sensor models further compounds this challenge. For instance, LiDAR sensors from manufacturers such as Leica, FARO, and Z + F differ in resolution, intensity calibration, and noise characteristics, which can significantly impact algorithm generalizability. Therefore, future studies should also focus on developing robust, generalized water leakage detection algorithms capable of maintaining stable performance across diverse datasets and sensor platforms.

7. Conclusions

Water leakage detection in shield tunnels is critical for ensuring the safety and operational integrity of underground infrastructure. This review systematically evaluates three primary sensing technologies, including photogrammetry, LiDAR, and infrared thermal imaging, highlighting their distinct advantages and limitations in practical applications. Photogrammetry excels in high-resolution visual inspections with broad coverage, though its effectiveness is compromised under suboptimal lighting and in occluded environments. LiDAR systems have emerged as highly effective solutions, providing precise 3D spatial and geometric data, essential for accurately localizing water leakage features in complex tunnel environments. In particular, LiDAR-based detection methodologies have been systematically categorized into grid-based, voxel-based, and point-based approaches. Grid-based methods transform point clouds into 2D intensity maps, significantly simplifying computation but losing spatial information. Voxel-based methods retain 3D structural relationships, enhancing spatial localization of water leakages at increased computational costs. Point-based methods fully preserve the original spatial information, allowing the high precision in water leakage detection. However, they require sophisticated analytical frameworks and computational resources. Infrared thermal imaging effectively identifies moisture-related thermal anomalies, although it is limited by low spatial resolution, sensitivity to environmental interference, and thermal properties of tunnel materials.

Furthermore, integrating advanced data-processing strategies, particularly deep learning and multimodal sensor fusion, has shown considerable promise for enhancing feature extraction, detection robustness, and overall accuracy. Future research should prioritize the development of integrated multi-sensor platforms, sophisticated multimodal data fusion techniques, and lightweight, real-time detection algorithms suitable for practical deployment. Additionally, significant attention must be directed towards improving algorithmic robustness and generalization across diverse sensor models and real-world environments.

To facilitate continued advancement in this field, we introduce and publicly release a comprehensive LiDAR-acquired point cloud dataset specifically created for tunnel water leakage detection. This dataset is intended to serve as a valuable resource to support methodological development and validation, ultimately contributing to more reliable and efficient tunnel maintenance strategies.

CRediT authorship contribution statement

Jundi Jiang: Writing – review & editing, Writing – original draft, Visualization, Validation, Methodology, Formal analysis, Data curation, Conceptualization. **Yueqian Shen:** Writing – review & editing, Validation, Supervision, Project administration, Methodology, Funding acquisition, Conceptualization. **Jinhu Wang:** Supervision, Project administration, Investigation, Formal analysis, Conceptualization.

Jinguo Wang: Supervision, Project administration, Investigation, Formal analysis, Conceptualization. **Junjun Huang:** Validation, Data curation. **Shihan Fu:** Data curation. **Kai Guo:** Project administration, Funding acquisition. **Vagner Ferreira:** Supervision, Project administration.

Declaration of competing interest

The authors declare that they have no known competing financial interests or personal relationships that could have appeared to influence the work reported in this paper.

Acknowledgement

This work was supported by the National Natural Science Foundation of China (Grant No. 41801379, 42201487, W2432026), the Open Found of Tunnel and Underground Engineering Research Center of Jiangsu Province (Grant No. 2023-SDJJ-01), and Guangdong Basic and Applied Basic Research Foundation (Grant No. 2023A1515011216). The authors are grateful to the High Performance Computing platform at Hohai University for processing the point cloud dataset in this paper.

Data availability

The dataset S3DIS_leakge in this study is publicly available at the following link: www.kaggle.com/datasets/yueqianshen/s3dis-leakage.

References

[1] Y.-J. Cheng, W. Qiu, J. Lei, Application of terrestrial laser scanning in tunnel inspection, Electron. J. Geotech. Eng. 21 (2016) 4683–4688.
[2] F. Gong, W. Wu, T. Li, X. Si, Experimental simulation and investigation of spalling failure of rectangular tunnel under different three-dimensional stress states, Int. J. Rock Mech. Min. Sci. 122 (2019) 104081.
[3] S. Wang, C. Liu, G. Ma, S. Cao, J. Zhang, D. Lu, C. He, Experimental investigation on the influence of regional concrete spalling on shield tunnel segments, Adv. Civ. Eng. 2019 (2019) 1829124.
[4] J. Liao, Y. Yue, D. Zhang, W. Tu, R. Cao, Q. Zou, Q. Li, Automatic tunnel crack inspection using an efficient mobile imaging module and a lightweight CNN, IEEE Trans. Intell. Transp. Syst. 23 (2022) 15190–15203.
[5] T. Yu, A. Zhu, Y. Chen, Efficient crack detection method for tunnel lining surface cracks based on infrared images, J. Comput. Civ. Eng. 31 (2017).
[6] L. Attard, C.J. Debono, G. Valentino, M. Di Castro, Tunnel inspection using photogrammetric techniques and image processing: a review, ISPRS J. Photogramm. Remote Sens. 144 (2018) 180–188.
[7] K. Wang, Z. Zhang, X. Wu, L. Zhang, Multi-class object detection in tunnels from 3D point clouds: an auto-optimized lazy learning approach, Adv. Eng. Inf. 52 (2022) 101543.
[8] Y. Song, C. Lu, X. Li, L. Zhao, X. Ye, T. Jin, Convergence deformation of existing shield tunnel induced by adjacent shield tunnelling construction, International Conference on Civil Engineering, Springer (2023) 382–389.
[9] C. Li, S. Hou, Y. Liu, P. Qin, F. Jin, Q. Yang, Analysis on the crown convergence deformation of surrounding rock for double-shield TBM tunnel based on advance borehole monitoring and inversion analysis, Tunn. Undergr. Space Technol. 103 (2020) 103513.
[10] K. Wang, X. Yao, Rapid detecting equipment for structural defects of metro tunnel, 6th International Symposium on Life-Cycle Civil Engineering (IALCCE), Ghent, BELGIUM, 2018, pp. 1561–1567.
[11] S. Liu, X. Xu, G. Jeon, J. Chen, B.-G. He, Deep learning based water leakage detection for shield tunnel lining, Front. Struct. Civ. Eng. (2024) 1–12.
[12] Q. Luo, B. Gao, W.L. Woo, Y. Yang, Temporal and spatial deep learning network for infrared thermal defect detection, NDT & E Int. 108 (2019) 102164.
[13] J. Liu, Z. Zhao, C. Lv, Y. Ding, H. Chang, Q. Xie, An image enhancement algorithm to improve road tunnel crack transfer detection, Constr. Build. Mater. 348 (2022).
[14] B. Wang, N. He, F. Xu, Y. Du, H. Xu, Visual detection method of tunnel water leakage diseases based on feature enhancement learning, Tunn. Undergr. Space Technol. 153 (2024) 106009.
[15] G. Kuang, B. Li, S. Mo, X. Hu, L. Li, Review on machine learning-based defect detection of shield tunnel lining, Periodica Polytechnica-Civil Engineering 66 (2022) 943–957.
[16] H. Huang, Y. Sun, Y. Xue, F. Wang, Inspection equipment study for subway tunnel defects by grey-scale image processing, Adv. Eng. Inf. 32 (2017) 188–201.
[17] H.-W. Huang, Q.-T. Li, D.-M. Zhang, Deep learning based image recognition for crack and leakage defects of metro shield tunnel, Tunn. Undergr. Space Technol. 77 (2018) 166–176.
[18] D. Li, Q. Xie, X. Gong, Z. Yu, J. Xu, Y. Sun, J. Wang, Automatic defect detection of metro tunnel surfaces using a vision-based inspection system, Adv. Eng. Inf. 47 (2021) 101206.
[19] Y. Xue, Y. Li, A fast detection method via region-based fully convolutional neural networks for shield tunnel lining defects, Comput. Aided Civ. Inf. Eng. 33 (2018) 638–654.
[20] S. Zhao, D.M. Zhang, H.W. Huang, Deep learning-based image instance segmentation for moisture marks of shield tunnel lining, Tunn. Undergr. Space Technol. 95 (2020).
[21] S. Zhao, M. Shadabfar, D. Zhang, J. Chen, H. Huang, Deep learning-based classification and instance segmentation of leakage-area and scaling images of shield tunnel linings, Struct. Control Health Monit. 28 (2021) e2732.
[22] Y. Tan, X. Li, J. Lai, J. Ai, Real-time tunnel lining leakage image semantic segmentation via multiple attention mechanisms, Meas. Sci. Technol. 35 (2024) 075204.
[23] L. Xu, Y. Wang, A. Dong, L. Zhu, H. Shi, Z. Yu, Image-based intelligent detection of typical defects of complex subway tunnel surface, Tunn. Undergr. Space Technol. 140 (2023) 105266.
[24] X. Wu, N. Guo, MGSLU-Net: a lightweight network for efficient detection of water leakage in subway tunnel linings, Vis. Comput. (2025) 1–14.
[25] M. Zhou, W. Cheng, H. Huang, J. Chen, A novel approach to automated 3D spalling defects inspection in railway tunnel linings using laser intensity and depth information, Sensors 21 (2021).
[26] O.E. Mora, A. Suleiman, J. Chen, D. Pluta, M.H. Okubo, R. Josenhans, Comparing sUAS photogrammetrically-derived point clouds with GNSS measurements and terrestrial laser scanning for topographic mapping, Drones 3 (2019).
[27] E. Kaartinen, K. Dunphy, A. Sadhu, LiDAR-based structural health monitoring: applications in civil infrastructure systems, Sensors 22 (2022).
[28] D. Anton, B. Medjdoub, R. Shrahily, J. Moyano, Accuracy evaluation of the semi-automatic 3D modeling for historical building information models, Int. J. Archit. Heritage 12 (2018) 790–805.
[29] Y. Shen, J. Wang, I. Puente, A novel baseline-based method to detect local structural changes in masonry walls using dense terrestrial laser scanning point clouds, IEEE Sens. J. 20 (2020) 6504–6515.
[30] J. Wang, X. Wei, W. Wang, J. Wang, J. Peng, S. Wang, Q. Zaheer, J. You, J. Xiong, S. Qiu, A multistation 3D point cloud automated global registration and accurate positioning method for railway tunnels, Struct. Control Hlth. 2023 (2023).
[31] N. Shen, B. Wang, H. Ma, X. Zhao, Y. Zhou, Z. Zhang, J. Xu, A review of terrestrial laser scanning (TLS)-based technologies for deformation monitoring in engineering, Measurement 223 (2023).
[32] H. Wang, Y. Liu, Q. Hu, B. Wang, J. Chen, Z. Dong, Y. Guo, W. Wang, B. Yang, RoReg: Pairwise point cloud registration with oriented descriptors and local rotations, IEEE Trans. Pattern Anal. Mach. Intell. 45 (2023) 10376–10393.
[33] T. Nuttens, C. Stal, H. De Backer, K. Schotte, P. Van Bogaert, A. De Wulf, Assessment of the tidal influences on tunnels based on different monitoring techniques: laser scanning, levelling and strain gauges, 6th International conference on Engineering Surveying (INGEO 2014), Slovenská Technická Univerzita v Bratislave. Stavebná Fakulta, 2014, pp. 223–228.
[34] S. Chen, B. Liu, C. Feng, C. Vallespi-Gonzalez, C. Wellington, 3D point cloud processing and learning for autonomous driving: impacting map creation, localization, and perception, IEEE Signal Process Mag. 38 (2021) 68–86.
[35] D.A.R. Williams, G. Matasci, N.C. Coops, S.E. Gergel, Object-based urban landcover mapping methodology using high spatial resolution imagery and airborne laser scanning, J. Appl. Remote Sens. 12 (2018).
[36] X. Han, C. Liu, Y. Zhou, K. Tan, Z. Dong, B. Yang, WHU-Urban3D: an urban scene LiDAR point cloud dataset for semantic instance segmentation, ISPRS J. Photogramm. Remote Sens. 209 (2024) 500–513.
[37] P. Li, Q. Wang, J. Li, Y. Pei, P. He, Automated extraction of tunnel leakage location and area from 3D laser scanning point clouds, Opt. Lasers Eng. 178 (2024) 108217.
[38] S. Liu, H. Sun, Z. Zhang, Y. Li, R. Zhong, J. Li, S. Chen, A multiscale deep feature for the instance segmentation of water leakages in tunnel using MLS point cloud intensity images, IEEE Trans. Geosci. Remote Sens. 60 (2022).
[39] L. Wang, S. Wang, Z. You, Spatially connected component analysis based 3d detection and visualization of subway tunnel lining water leakage using mls data, Available at SSRN 4892163, 2024.
[40] H. Sun, Z. Xu, L. Yao, R. Zhong, L. Du, H. Wu, Tunnel monitoring and measuring system using mobile laser scanning: Design and deployment, Remote Sens. 12 (2020) 730.
[41] H. Sun, S. Liu, R. Zhong, L. Du, Cross-section deformation analysis and visualization of shield tunnel based on mobile tunnel monitoring system, Sensors 20 (2020) 1006.
[42] L. Han, J. Chen, H. Li, G. Liu, B. Leng, A. Ahmed, Z. Zhang, Multispectral water leakage detection based on a one-stage anchor-free modality fusion network for metro tunnels, Autom. Constr. 140 (2022).
[43] W. Kang, L. Gaohang, H. Bo, Z. Hanming, L. Jian, Study on the distribution patterns of temperature fields and thermal image feature enhancement in tunnel lining cracks and leakage, J. Nondestr. Eval. 44 (2025) 22.
[44] M.S. Jadin, S. Taib, Recent progress in diagnosing the reliability of electrical equipment by using infrared thermography, Infrared Phys. Technol. 55 (2012) 236–245.
[45] Z. Lu, F. Zhu, L. Shi, F. Wang, P. Zeng, J. Hu, X. Liu, Y. Xu, Q. Chen, Automatic seepage detection in cable tunnels using infrared thermography, Meas. Sci. Technol. 30 (2019).

[46] M. Sun, X. Xu, D. Zhou, J. Li, X. He, Synchronous acquisition control system and coordinate correction algorithm for subway tunnel comprehensive detection equipment, IEEE Sens. J. (2024).
[47] Y. Xue, X. Cai, M. Shadabfar, H. Shao, S. Zhang, Deep learning-based automatic recognition of water leakage area in shield tunnel lining, Tunn. Undergr. Space Technol. 104 (2020).
[48] J. Chen, X. Xu, G. Jeon, D. Camacho, B.-G. He, WLR-Net: an improved YOLO-V7 with edge constraints and attention mechanism for water leakage recognition in the tunnel, IEEE Trans. Emerging Top. Comput. Intell. (2024).
[49] I. Armeni, S. Sax, A.R. Zamir, S. Savarese, Joint 2d-3d-semantic data for indoor scene understanding, arXiv preprint arXiv:1702.01105, 2017.
[50] X.W. Gao, S. Li, B.Y. Jin, M. Hu, W. Ding, Intelligent crack damage detection system in shield tunnel using combination of retinanet and optimal adaptive selection, J. Intell. Fuzzy Syst. 40 (2021) 4453–4469.
[51] H. Huang, S. Zhao, D. Zhang, J. Chen, Deep learning-based instance segmentation of cracks from shield tunnel lining images, Struct. Infrastruct. Eng. 18 (2022) 183–196.
[52] S. Zhao, D. Zhang, Y. Xue, M. Zhou, H. Huang, A deep learning-based approach for refined crack evaluation from shield tunnel lining images, Autom. Constr. 132 (2021).
[53] S. Konishi, K. Kawakami, M. Taguchi, Inspection method with infrared thermometry for detect void in subway tunnel lining, 15th World Conference of the Associated Research Centers for the Urban Underground Space - Underground Urbanization as a Prerequisite for Sustainable Development (ACUUS), St Petersburg, RUSSIA, 2016, pp. 474–483.
[54] Z. Yin, Z. Lei, A. Zheng, J. Zhu, X.-Z. Liu, Automatic detection and association analysis of multiple surface defects on shield subway tunnels, Sensors 23 (2023).
[55] C. Liu, J. Lai, Q. Li, A review of research situation on shield tunnel diseases, 2nd International Conference on Civil Engineering, Architecture and Sustainable Infrastructure (ICCEASI 2013), Zhengzhou, PEOPLES R CHINA, 2013, pp. 943–948.
[56] J. Canny, A computational approach to edge detection, IEEE Trans. Pattern Anal. Mach. Intell. 679–698 (1986).
[57] N. Kanopoulos, N. Vasanthavada, R.L. Baker, Design of an image edge detection filter using the Sobel operator, IEEE J. Solid-State Circuits 23 (1988) 358–367.
[58] T. Dawood, Z. Zhu, T. Zayed, Computer vision-based model for moisture marks detection and recognition in subway networks, J. Comput. Civ. Eng. 32 (2018).
[59] N. Otsu, A threshold selection method from gray-level histograms, Automatica 11 (1975) 23–27.
[60] L. Lu, M. Ji, X. Wen, Y. Xiang, An empirical study on construction emergency disaster management and risk assessment in shield tunnel construction project with big data analysis, Int. J. Data Min. Bioinf. 28 (2024).
[61] X. Yadong, J. Fei, G. Chunsheng, G. Yongfa, L. Jie, Deep learning-based shield tunnel leakage mixed dataset construction and fine segmentation, 2024.
[62] J. Long, E. Shelhamer, T. Darrell, Ieee, Fully convolutional networks for semantic segmentation, IEEE Conference on Computer Vision and Pattern Recognition (CVPR), Boston, MA, 2015, pp. 3431–3440.
[63] J. Redmon, S. Divvala, R. Girshick, A. Farhadi, Ieee, you only look once: unified, real-time object detection, in: 2016 IEEE Conference on Computer Vision and Pattern Recognition (CVPR), Seattle, WA, 2016, pp. 779–788.
[64] L.-C. Chen, Y. Zhu, G. Papandreou, F. Schroff, H. Adam, Encoder-decoder with atrous separable convolution for semantic image segmentation, 15th European Conference on Computer Vision (ECCV), Munich, GERMANY, 2018, pp. 833–851.
[65] K. He, G. Gkioxari, P. Dollar, R. Girshick, Mask R-CNN, IEEE Trans. Pattern Anal. Mach. Intell. 42 (2020) 386–397.
[66] S. Ren, K. He, R. Girshick, J. Sun, Faster R-CNN: towards real-time object detection with region proposal networks, IEEE Trans. Pattern Anal. Mach. Intell. 39 (2017) 1137–1149.
[67] S.J. Feng, Y. Feng, X.L. Zhang, Y.H. Chen, Deep learning with visual explanations for leakage defect segmentation of metro shield tunnel, Tunn. Undergr. Space Technol. 136 (2023).
[68] Y. Xue, F. Jia, X. Cai, M. Shadabfar, H. Huang, An optimization strategy to improve the deep learning-based recognition model of leakage in shield tunnels, Comput. Aided Civ. Inf. Eng. 37 (2022) 386–402.
[69] Q. Zhao, C. Wu, W. Wu, Recognition method of subway tunnel leakage diseases based on semantic segmentation, International Conference on Image, Signal Processing, and Pattern Recognition (ISPP 2024), SPIE, 2024, pp. 1374-1381.
[70] Y. Wu, M. Hu, G. Xu, X. Zhou, Z. Li, Detecting leakage water of shield tunnel segments based on mask R-CNN, in: 2019 IEEE International Conference on Architecture, Construction, Environment and Hydraulics (ICACEH), IEEE, 2019, pp. 25–28.
[71] D. Wang, G. Hou, Q. Chen, W. Li, H. Li, Y. Shao, X. Yu, Automatic recognition of tunnel water leakage based on adaptive information extraction network and multiscale feature enhancement module, IEEE Access (2024).
[72] L. Lin, H. Zhu, Y. Ma, Y. Peng, Y. Xia, Surface feature and defect detection method for shield tunnel based on deep learning, J. Comput. Civ. Eng. 39 (2025) 04025019.
[73] W. Wang, X. Xu, H. Yang, Intelligent detection of tunnel leakage based on improved Mask R-CNN, Symmetry-Basel 16 (2024).
[74] Y. Xu, D. Li, Q. Xie, Q. Wu, J. Wang, Automatic defect detection and segmentation of tunnel surface using modified Mask R-CNN, Measurement 178 (2021) 109316.
[75] L. Tan, X. Hu, T. Tang, D. Yuan, A lightweight metro tunnel water leakage identification algorithm via machine vision, Eng. Fail. Anal. 150 (2023).
[76] H. Zhao, J. Shi, X. Qi, X. Wang, J. Jia, Pyramid scene parsing network, IEEE Computer Vision and Pattern Recognition (CVPR) 2017 (2017) 2881–2890.
[77] W. Sun, S. Hou, G. Wu, D. Feng, J. Fan, Image-based automatic multiple-defect detection of urban utility tunnel using UUTNet, Adv. Struct. Eng. 27 (2024) 1170–1188.
[78] M. Tan, Efficientnet: Rethinking model scaling for convolutional neural networks, arXiv preprint arXiv:1905.11946, 2019.
[79] Z. Zhou, J. Zhang, C. Gong, Automatic detection method of tunnel lining multi-defects via an enhanced you only look once network, Comput. Aided Civ. Inf. Eng. 37 (2022) 762–780.
[80] D. Qiu, H. Liang, Z. Wang, Y. Tong, S. Wan, Hybrid-supervised-learning-based automatic image segmentation for water leakage in subway tunnels, Appl. Sci.-Basel 12 (2022).
[81] X. Gao, M. Jian, M. Hu, M. Tanniru, S. Li, Faster multi-defect detection system in shield tunnel using combination of FCN and faster RCNN, Adv. Struct. Eng. 22 (2019) 2907–2921.
[82] W. Wang, C. Su, G. Han, Y. Dong, Efficient segmentation of water leakage in shield tunnel lining with convolutional neural network, Struct. Health Monit.- Int. J. 23 (2024) 671–685.
[83] N. Ma, X. Zhang, H.-T. Zheng, J. Sun, Shufflenet v2: Practical guidelines for efficient cnn architecture design, in: Proceedings of the European Conference on Computer Vision (ECCV), 2018, pp. 116–131.
[84] Z. Gan, L. Teng, Y. Chang, X. Feng, M. Gao, X. Gao, A multi-information fusion method for repetitive tunnel disease detection, Sustainability 16 (2024) 4285.
[85] Y. Feng, S.-J. Feng, X.-L. Zhang, D.-M. Zhang, Y. Zhao, A two-step deep learning-based framework for metro tunnel lining defect recognition, Tunn. Undergr. Space Technol. 150 (2024) 105832.
[86] J. Chen, X. Yu, S. Liu, T. Chen, W. Wang, G. Jeon, B. He, Tunnel SAM adapter: Adapting segment anything model for tunnel water leakage inspection, Geohazard Mechanics 2 (2024) 29–36.
[87] Y. Shen, J. Huang, J. Wang, J. Jiang, J. Li, V. Ferreira, A review and future directions of techniques for extracting powerlines and pylons from LiDAR point clouds, Int. J. Appl. Earth Obs. Geoinf. 132 (2024) 104056.
[88] N. Sanchiz-Viel, E. Bretagne, E.M. Mouaddib, P. Dassonvalle, Radiometric correction of laser scanning intensity data applied for terrestrial laser scanning, ISPRS J. Photogramm. Remote Sens. 172 (2021) 1–16.
[89] K. Tan, X. Cheng, Q. Ju, S. Wu, Correction of mobile TLS intensity data for water leakage spots detection in metro tunnels, IEEE Geosci. Remote Sens. Lett. 13 (2016) 1711–1715.
[90] S. Kaasalainen, A. Jaakkola, M. Kaasalainen, A. Krooks, A. Kukko, Analysis of incidence angle and distance effects on terrestrial laser scanner intensity: search for correction methods, Remote Sens. 3 (2011) 2207–2221.
[91] A. Kukko, S. Kaasalainen, P. Litkey, Effect of incidence angle on laser scanner intensity and surface data, Appl. Opt. 47 (2008) 986–992.
[92] A. Krooks, S. Kaasalainen, T. Hakala, O. Nevalainen, Correction of intensity incidence angle effect in terrestrial laser scanning, ISPRS Ann. Photogramm. Remote Sens. Spatial Inf. Sci. 2 (2013) 145–150.
[93] B. Höfle, N. Pfeifer, Correction of laser scanning intensity data: data and model-driven approaches, ISPRS J. Photogramm. Remote Sens. 62 (2007) 415–433.
[94] A.G. Kashani, M.J. Olsen, C.E. Parrish, N. Wilson, A review of LiDAR radiometric processing: from ad hoc intensity correction to rigorous radiometric calibration, Sensors 15 (2015) 28099–28128.
[95] T. Xu, L. Xu, X. Li, J. Yao, Detection of water leakage in underground tunnels using corrected intensity data and 3D point cloud of terrestrial laser scanning, IEEE Access 6 (2018) 32471–32480.
[96] K. Tan, X. Cheng, Q. Ju, Combining mobile terrestrial laser scanning geometric and radiometric data to eliminate accessories in circular metro tunnels, J. Appl. Remote Sens. 10 (2016) 030503.
[97] W. Fang, X. Huang, F. Zhang, D. Li, Intensity correction of terrestrial laser scanning data by estimating laser transmission function, IEEE Trans. Geosci. Remote Sens. 53 (2015) 942–951.
[98] A.F.C. Errington, B.L.F. Daku, A.F. Prugger, Ieee, Reflectance modelling using terrestrial LiDAR intensity data, IEEE International Conference on Imaging Systems and Techniques (IST), Macau, Peoples R China, 2015, pp. 27-32.
[99] K. Tan, X. Cheng, Surface reflectance retrieval from the intensity data of a terrestrial laser scanner, J. Opt. Soc. Am. A-Opt. Image Sci. Vision 33 (2016) 771–778.
[100] T. Xu, L. Xu, B. Yang, X. Li, J. Yao, Terrestrial laser scanning intensity correction by piecewise fitting and overlap-driven adjustment, Remote Sens. 9 (2017).
[101] E. Bretagne, P. Dassonvalle, G. Caron, Spherical target-based calibration of terrestrial laser scanner intensity. Application to colour information computation, ISPRS J. Photogramm. Remote Sens. 144 (2018) 14–27.
[102] H. Cui, X. Ren, Q. Mao, Q. Hu, W. Wang, Shield subway tunnel deformation detection based on mobile laser scanning, Autom. Constr. 106 (2019).
[103] Z. Guo, J. Wei, H. Sun, R. Zhong, C. Ji, Enhanced water leakage detection in shield tunnels based on laser scanning intensity images using RDES-Net, IEEE J. Sel. Top. Appl. Earth Obs. Remote Sens. (2024).
[104] H. Huang, W. Cheng, M. Zhou, J. Chen, S. Zhao, Towards automated 3D inspection of water leakages in shield tunnel linings using mobile laser scanning data, Sensors 20 (2020).
[105] Z. Yin, Z. Lei, A. Zheng, J. Zhu, X.-Z. Liu, Automatic detection and association analysis of multiple surface defects on shield subway tunnels, Sensors 23 (2023) 7106.
[106] Z. Zhang, A. Ji, K. Wang, L. Zhang, UnrollingNet: an attention-based deep learning approach for the segmentation of large-scale point clouds of tunnels, Autom. Constr. 142 (2022).

[107] Q. Chen, Z. Kang, Z. Cao, X. Xie, B. Guan, Y. Pan, J. Chang, Combining cylindrical voxel and Mask R-CNN for automatic detection of water leakages in shield tunnel point clouds, Remote Sens. 16 (2024).
[108] Y. Liu, R. Zhong, W. Chen, H. Sun, Y. Ren, N. Lei, Study of tunnel surface parameterization of 3-D laser point cloud based on harmonic map, IEEE Geosci. Remote Sens. Lett. 17 (2020) 1623–1627.
[109] S. Kaasalainen, H. Niittymaki, A. Krooks, K. Koch, H. Kaartinen, A. Vain, H. Hyyppa, Effect of target moisture on laser scanner intensity, IEEE Trans. Geosci. Remote Sens. 48 (2009) 2128–2136.
[110] C. Suchocki, M. Damięcka-Suchocka, J. Katzer, J. Janicka, J. Rapiński, P. Stałowska, Remote detection of moisture and bio-deterioration of building walls by time-of-flight and phase-shift terrestrial laser scanners, Remote Sens. 12 (2020) 1708.
[111] C. Suchocki, J. Katzer, J. Rapiński, Terrestrial laser scanner as a tool for assessment of saturation and moisture movement in building materials, Periodica Polytechnica Civ. Eng. 62 (2018) 694–699.
[112] Y. Xue, P. Shi, F. Jia, H. Huang, 3D reconstruction and automatic leakage defect quantification of metro tunnel based on SfM-Deep learning method, Underground Space 7 (2022) 311–323.
[113] J. Qian, F. Xue, T. Wang, Z. Lin, M. Cai, F. Shou, Combining SfM and deep learning to construct 3D point cloud models of shield tunnels and Realize spatial localization of water leakages, Measurement 250 (2025) 117114.
[114] X. Cheng, X. Hu, K. Tan, L. Wang, L. Yang, Automatic detection of shield tunnel leakages based on terrestrial mobile LiDAR intensity images using deep learning, IEEE Access 9 (2021) 55300–55310.
[115] Z. Zhang, A. Ji, L. Zhang, Y. Xu, Q. Zhou, Deep learning for large-scale point cloud segmentation in tunnels considering causal inference, Autom. Constr. 152 (2023) 104915.
[116] H. Wu, Q. Zhu, Y. Guo, W. Zheng, L. Zhang, Q. Wang, R. Zhou, Y. Ding, W. Wang, S. Pirasteh, M. Liu, Multi-level voxel representations for digital twin models of tunnel geological environment, Int. J. Appl. Earth Obs. Geoinf. 112 (2022).
[117] A. Ji, A.W.Z. Chew, X. Xue, L. Zhang, An encoder-decoder deep learning method for multi-class object segmentation from 3D tunnel point clouds, Autom. Constr. 137 (2022).
[118] W. Lin, P. Li, X. Xie, A novel detection and assessment method for operational defects of pipe jacking tunnel based on 3D longitudinal deformation curve: a case study, Sensors 22 (2022).
[119] X. Xie, H. Tian, B. Zhou, K. Li, The life-cycle development and cause analysis of large diameter shield tunnel convergence in soft soil area, Tunn. Undergr. Space Technol. 107 (2021) 103680.
[120] J. Jiang, Y. Shen, J. Wang, Y. Zang, W. Wu, J. Wang, J. Li, V. Ferreira, Boosted bagging: a hybrid ensemble deep learning framework for point cloud semantic segmentation of shield tunnel leakage, Tunn. Undergr. Space Technol. 164 (2025) 106842.
[121] R.B. Rusu, N. Blodow, M. Beetz, Fast point feature histograms (FPFH) for 3D registration, 2009 IEEE international conference on robotics and automation, IEEE (2009) 3212–3217.
[122] J. Jiang, Y. Shen, J. Wang, J. Wang, C. Zhang, J. Wang, V. Ferreira, GEPT-Net: an efficient geometry enhanced point transformer for shield tunnel leakage segmentation, ISPRS J. Photogramm. Remote Sens. 221 (2025) 20–43.
[123] P. Yu, H. Wu, C. Liu, Z. Xu, Water leakage diagnosis in metro tunnels by intergration of laser point cloud and infrared thermal imaging, Int. Arch. Photogramm. Remote. Sens. Spat. Inf. Sci. 42 (2018) 2167–2171.
[124] J. Li, Z. Zhang, H. Sun, S. Xie, J. Zou, C. Ji, Y. Lu, X. Ren, L. Wang, GL-Net: Semantic segmentation for point clouds of shield tunnel via global feature learning and local feature discriminative aggregation, ISPRS J. Photogramm. Remote Sens. 199 (2023) 335–349.
[125] H. Cui, J. Li, Q. Mao, Q. Hu, C. Dong, Y. Tao, STSD: a large-scale benchmark for semantic segmentation of subway tunnel point cloud, Tunn. Undergr. Space Technol. 150 (2024) 105829.
[126] C. Yi, D. Lu, Q. Xie, S. Liu, H. Li, M. Wei, J. Wang, Hierarchical tunnel modeling from 3D raw LiDAR point cloud, Comput.-Aided Des. 114 (2019) 143–154.
[127] T. Inagaki, Y. Okamoto, Diagnosis of the leakage point on a structure surface using infrared thermography in near ambient conditions, NDT & E Int. 30 (1997) 135–142.
[128] M. Yahia, R. Gawai, T. Ali, M.M. Mortula, L. Albasha, T. Landolsi, Non-destructive water leak detection using multitemporal infrared thermography, IEEE Access 9 (2021) 72556–72567.
[129] D. Wang, G. Hou, Q. Chen, W. Li, H. Fu, X. Sun, X. Yu, Segmentation of tunnel water leakage based on a lightweight DeepLabV3+ model, Meas. Sci. Technol. 36 (2024) 015414.
[130] S. Qin, T. Qi, T. Deng, X. Huang, Image segmentation using vision transformer for tunnel defect assessment, Comput. Aided Civ. Inf. Eng. 39 (2024) 3243–3268.
[131] P.-S. Wang, Octformer: Octree-based transformers for 3d point clouds, ACM Transactions on Graphics (TOG) 42 (2023) 1–11.
[132] X. Liu, X. Liu, Y.S. Liu, Z. Han, SPU-Net: Self-supervised point cloud upsampling by coarse-to-fine reconstruction with self-projection optimization, IEEE Trans. Image Process. 31 (2022) 4213–4226.
[133] B. Peng, X. Wu, L. Jiang, Y. Chen, H. Zhao, Z. Tian, J. Jia, OA-CNNs: Omni-adaptive sparse CNNs for 3D semantic segmentation, in: Proceedings of the IEEE/CVF Conference on Computer Vision and Pattern Recognition, 2024, pp. 21305–21315.
[134] R.B. Rusu, N. Blodow, Z.C. Marton, M. Beetz, Aligning point cloud views using persistent feature histograms, 2008 IEEE/RSJ international conference on intelligent robots and systems, IEEE (2008) 3384–3391.
[135] F. Tombari, S. Salti, L. Di Stefano, Unique signatures of histograms for local surface description, 2010 European Conference on Computer Vision (ECCV), Springer (2010) 356–369.
[136] Z. Liu, X. Gao, Y. Yang, L. Xu, S. Wang, N. Chen, Z. Wang, Y. Kou, EDT-Net: a lightweight tunnel water leakage detection network based on LiDAR point clouds intensity images, IEEE J. Sel. Top. Appl. Earth Obs. Remote Sens. (2025).
[137] A. Zheng, S. Qi, Y. Cheng, D. Wu, J. Zhu, Efficient detection of apparent defects in subway tunnel linings based on deep learning methods, Appl. Sci. 14 (2024) 7824.
[138] K. Wang, X. Wu, H. Li, F. Wang, L. Zhang, H. Chen, Adaptively unsupervised seepage detection in tunnels from 3D point clouds, Struct. Infrastruct. Eng. (2022).